

### **OPEN ACCESS**

EDITED BY Christian Lønborg, Aarhus University, Denmark

REVIEWED BY

Víctor Fernández-Juárez, University of Copenhagen, Denmark Jonathan David Todd, University of East Anglia, United Kingdom Graham Barry Jones, Southern Cross University, Australia

\*CORRESPONDENCE Rafel Simó ☑ rsimo@icm.csic.es

### <sup>†</sup>PRESENT ADDRESSES

Pablo Rodríguez-Ros, Marilles Foundation, Palma, Mallorca, Illes Balears, Spain Stephanie G. Gardner, School of Life and Environmental Sciences, The University of Sydney, NSW, Australia Kristin Bergauer, Ocean Ecosystems Biology Unit, GEOMAR Helmholtz Centre for Ocean Research, Kiel. Germany

RECEIVED 20 November 2023 ACCEPTED 30 January 2024 PUBLISHED 16 February 2024

### CITATION

Masdeu-Navarro M, Mangot J-F, Xue L, Cabrera-Brufau M, Kieber DJ, Rodríguez-Ros P, Gardner SG, Bergauer K, Herndl GJ, Marrasé C and Simó R (2024) Diel variation of seawater volatile organic compounds, DMSP-related compounds, and microbial plankton inside and outside a tropical coral reef ecosystem. *Front. Mar. Sci.* 11:1341619. doi: 10.3389/fmars.2024.1341619

### COPYRIGHT

© 2024 Masdeu-Navarro, Mangot, Xue, Cabrera-Brufau, Kieber, Rodríguez-Ros, Gardner, Bergauer, Herndl, Marrasé and Simó. This is an open-access article distributed under the terms of the Creative Commons Attribution License (CC BY). The use, distribution or reproduction in other forums is permitted, provided the original author(s) and the copyright owner(s) are credited and that the original publication in this journal is cited, in accordance with accepted academic practice. No use, distribution or reproduction is permitted which does not comply with these terms.

# Diel variation of seawater volatile organic compounds, DMSP-related compounds, and microbial plankton inside and outside a tropical coral reef ecosystem

Marta Masdeu-Navarro<sup>1</sup>, Jean-François Mangot<sup>1</sup>, Lei Xue<sup>2</sup>, Miguel Cabrera-Brufau<sup>1</sup>, David J. Kieber<sup>2</sup>, Pablo Rodríguez-Ros<sup>1†</sup>, Stephanie G. Gardner<sup>1†</sup>, Kristin Bergauer<sup>3,4†</sup>, Gerhard J. Herndl<sup>3,4</sup>, Cèlia Marrasé<sup>1</sup> and Rafel Simó<sup>1\*</sup>

<sup>1</sup>Institut de Ciències del Mar (ICM-CSIC), Barcelona, Catalonia, Spain, <sup>2</sup>Department of Chemistry, College of Environmental Science and Forestry, State University of New York, Syracuse, NY, United States, <sup>3</sup>Department of Functional and Evolutionary Ecology, Bio-Oceanography and Marine Biology Unit, University of Vienna, Vienna, Austria, <sup>4</sup>NIOZ, Department of Marine Microbiology and Biogeochemistry, Royal Netherlands Institute for Sea Research, Den Burg, Netherlands

Biogenic volatile organic compounds (VOCs) play key roles in coral reef ecosystems, where, together with dimethylated sulfur compounds, they are indicators of ecosystem health and are used as defense strategies and infochemicals. Assessment and prediction of the exchange rates of VOCs between the oceans and atmosphere, with implications for atmospheric reactivity and climate, are hampered by poor knowledge of the regulating processes and their temporal variability, including diel cycles. Here, we measured the variation over 36h of the concentrations of DMSPCs (dimethylsulfoniopropionate (DMSP)-related compounds, namely DMSP, dimethylsulfoxide, acrylate, dimethylsulfide, and methanethiol as dimethyl disulfide) and VOCs (COS, CS<sub>2</sub>, isoprene, the iodomethanes CH<sub>3</sub>I and CH<sub>2</sub>CII, and the bromomethanes CHBr3 and CH2Br2), in surface waters inside the shallow, northern coral-reef lagoon of Mo'orea (French Polynesia) and 4 km offshore, in the tropical open ocean. Comparisons with concurrent measurements of sea surface temperature, solar radiation, biogeochemical variables (nutrients, organic matter), and the abundances and taxonomic affiliations of microbial plankton were conducted with the aim to explain interconnections between DMSPCs, VOCs, and their environment across diel cycles. In open ocean waters, deeper surface mixing and low nutrient levels resulted in low phytoplankton biomass and bacterial activity. Consequently, the diel patterns of VOCs were more dependent on photochemical reactions, with daytime increases for several compounds including dissolved dimethylsulfoxide, COS, CS<sub>2</sub>, CH<sub>3</sub>I, and CH<sub>2</sub>CII. A eukaryotic phytoplankton assemblage dominated by dinoflagellates and haptophytes provided higher cell-associated DMSP concentrations, yet the occurrence of DMSP degradation products (dimethylsulfide, dimethyl disulfide) was limited by photochemical loss. Conversely, in the shallow back reef lagoon the proximity of seafloor

sediments, corals and abundant seaweeds resulted in higher nutrient levels, more freshly-produced organic matter, higher bacterial activity, and larger algal populations of *Mamiellales*, diatoms and *Cryptomonadales*. Consequently, DMSP and dimethylsulfoxide concentrations were lower but those of most VOCs were higher. A combination of photobiological and photochemical processes yielded sunny-daytime increases and nighttime decreases of dimethylsulfide, dimethyl disulfide, COS, isoprene, iodomethanes and bromomethanes. Our results illustrate the important role of solar radiation in DMSPC and VOC cycling, and are relevant for the design of sampling strategies that seek representative and comparable measurements of these compounds.

KEYWORDS

coral reef, Mo'orea, tropical ocean, diel cycles, DMSP, VOC, solar radiation, microorganisms

# Introduction

Marine environments produce and emit volatile organic compounds (VOCs) mainly through biological and photochemical processes. Ocean-leaving VOCs participate in the regulation of atmospheric oxidative capacity and aerosol formation and growth in the low marine atmosphere (Carpenter et al., 2012). In the tropical oceans, furthermore, strong and deep convection rapidly transports ocean-emitted VOCs from the boundary layer to the upper troposphere and even the stratosphere, where they participate in ozone destruction and new aerosol formation (Fuhlbrügge et al., 2016; Lennartz et al., 2017; Williamson et al., 2019; Filus et al., 2020).

Tropical coral reefs are highly productive ecosystems in oligotrophic oceans (Hoegh-Guldberg et al., 2017) that harbor around 30% of all marine species (Knowlton et al., 2010). Scleractinian or stony corals, which form massive calcium carbonate skeletons, are the main builders of coral reefs, where they provide habitats to a variety of life forms, from vertebrate and invertebrate animals to seaweeds and planktonic and benthic microbes. Active recycling of nutrients in the entire ecosystem allows coral reefs to remain productive, provide ecological niches, and contribute to regional biogeochemical cycles. Coral reef ecosystems produce multiple VOCs (Exton et al., 2015; Masdeu-Navarro et al., 2022) that are indicators of the ecosystem state and chemical cues for organism interactions and/or defense strategies. It has been suggested that coral reefs are hot spots of VOC production and emission, but the evidence is limited (Exton et al., 2015), and the statement cannot be generalized (Masdeu-Navarro et al., 2022).

Only a few studies have characterized the VOC composition of reef ecosystems beyond dimethylsulfide (DMS) and isoprene (Lawson et al., 2020; 2021; Masdeu-Navarro et al., 2022), and knowledge of their sources is largely uneven across compounds. Isoprene (C<sub>5</sub>H<sub>8</sub>) is produced by phytoplankton (McGenity et al.,

2018) and tropical coral holobionts (Swan et al., 2016; Dawson et al., 2021; Lawson et al., 2021); whether its production results from thermal stress, as is the case with vascular plants on land (Loreto and Schnitzler, 2010; McGenity et al., 2018), is unknown. Halomethanes (halogenated C1 compounds) are also produced by phytoplankton and consequently ubiquitous in the surface ocean, but they typically occur at much higher concentrations in coastal waters, where they are produced by seaweeds in response to oxidative stress and as part of defense mechanisms (Carpenter et al., 2012). Amongst volatile sulfur compounds, carbonyl sulfide (COS) is mostly generated by the interaction of solar radiation with dissolved organic matter (Uher and Andreae, 1997; Lennartz et al., 2020). Carbon disulfide (CS<sub>2</sub>) is thought to be produced by hypoxic sediments at the seafloor and photochemical reactions in sunlit waters, yet the mechanisms are not well characterized (Kim and Andreae, 1992; Lennartz et al., 2020). More is known about DMS and its pervasive biochemical precursor, the non-volatile compound dimethylsulfoniopropionate (DMSP). Marine environments, including coral reefs, are sources of DMSP because many microalgal taxa, including both phytoplankton and the coral endosymbionts Symbiodiniaceae, synthesize vast amounts of DMSP as a cellular osmolyte and antioxidant (Deschaseaux et al., 2014), and so do some cnidarians (Raina et al., 2013) and their associated bacteria (Kuek et al., 2022). DMSP can undergo enzymatic cleavage, resulting in the formation of DMS and acrylate. This catabolic pathway is believed to play a pivotal role in mitigating oxidative stress (Sunda et al., 2002; McParland et al., 2021). An alternative, often preferential, catabolic process involves demethylation and demethiolation, leading to the assimilation of sulfur by the consumer and the release of methanethiol (MeSH) as a by-product (Kiene et al., 2000; Howard et al., 2006). Subsequent oxidation of DMS and MeSH gives rise to dimethylsulfoxide (DMSO) and dimethyldisulfide (DMDS), respectively (Kiene, 1996; Del Valle et al., 2007). DMSO can also be produced by

cleavage of dimethylsulfoxonium propionate (DMSOP), a metabolite produced by intracellular oxidation of DMSP (Thume et al., 2018). The suite of DMSP, DMS, MeSH, DMDS, acrylate and DMSO can be collectively named DMSP-related compounds (DMSPCs).

Even though solar radiation represents a fundamental driver for the production and cycling of many VOCs and DMSPCs (Carpenter et al., 2012), changes in the concentrations of these compounds over diel cycles are largely unknown. Very few studies have addressed diel cycles in any marine ecosystem, including the open ocean, and they have mainly focused on DMSPCs (Broadbent and Jones, 2006; Galí et al., 2013b; Royer et al., 2016). Diel variations are expected in coral reefs because of the high densities of light-sensitive organisms. Coral holobiont physiology changes in response to incident solar radiation and circadian rhythms (Hemond and Vollmer, 2015), and switches from daytime autotrophy, when the algal symbionts fix carbon and produce oxygen, to nighttime heterotrophy, when polyps prey on plankton (Hoadley et al., 2021) and animal respiration is higher due to digestion (Schneider et al., 2009). In a previous paper (Masdeu-Navarro et al., 2022), we reported for the first time the diel patterns of VOCs and DMSPCs in the close vicinity (1-2 cm) and 2 m away from a patch of the coral Acropora pulchra in a reef at the NW coast of Mo'orea, French Polynesia. We showed that the coral holobiont was a strong source of DMSPCs, with large daytime release suggesting that these compounds arose from solar radiation stress. Conversely, the coral was a weaker or null source of other volatile sulfur compounds, isoprene and halomethanes. Here we investigated the short-term variations of VOCs and DMSPCs concentrations over day and night in the lagoon waters of another Mo'orean reef and compare it with the short-term variations in the neighboring open ocean. We hypothesized that (a) microbial plankton and solar radiation govern the presence and dynamics of VOCs and DMSPCs in the open ocean, while in the back reef these compounds are also controlled by corals, seaweeds, sediments, and photochemical reactions with freshly produced organic matter; (b) in both cases, solar radiation plays a pivotal role, resulting in recognizable diel patterns for these compounds. Our overarching goal was to shed light on the origin of these compounds in tropical marine ecosystems, their short-term variability, and their dependence on sunlight.

# Materials and methods

# Study area

Fieldwork was conducted in the northern coast of the island of Mo'orea, French Polynesia (17°29'00.0"S 149°50'00.0"W), between 12th and 20th of April 2018. Surface water was collected at two sampling sites: one located 4 km offshore in the open ocean (OO) over a bathymetric depth of 1200 m; and the other located in the back-reef (BR) lagoon, over a depth of ~2.5 m. The northern reefs of Moorea have shallow depths (0.5-3 m; Leichter et al., 2013) and

are characterized by patches of *Pocillopora* spp., *Acropora* spp. and other corals on a sandy bottom, and partly covered by the brown seaweed *Turbinaria ornata* (Masdeu-Navarro et al., 2022).

# Sample collection and storage

At each of the two sites, seawater samples were collected every 6 h over a period of 34 h on April 12-13 (BR) and April 19-20 (OO) from the surface (0-50 cm) using a small boat. Sampling times were 04:00, 10:00, 16:00, 22:00, 04:00, 10:00, and 14:00 (13:00 at OO) local time. Logistical and personnel limitations prevented extending the sampling to another 24-h cycle, which would have been desirable to ensure that the observed patterns were repeated. For VOCs, DMSPCs, and dissolved organic carbon and nitrogen (DOC, DON), samples were collected using acid-cleaned 0.5 L glass bottles rinsed three times and filled to the brim by hand. For other biogeochemical variables, cell counts and 16S and 18S genes rRNA metabarcoding, water was withdrawn with a peristaltic pump into an acid-cleaned and pre-rinsed Teflon-lined plastic carboy (20 L), while filtered through a 200 µm mesh to remove large particles and organisms. Samples were maintained in a water bath continuously flushed with surface seawater, in dimmed light, until processing in the UC Berkeley Gump laboratory on the island ca. 1 h after collection.

# **VOC and DMSPC concentrations**

Dissolved VOCs were quantified within 3 h of sample collection by purge and trap gas chromatography-mass spectrometry as described previously (Masdeu-Navarro et al., 2022). Target VOCs were COS, DMS, CS2, DMDS, isoprene, CH3I, CH2CII, CH2Br2, CHBr<sub>3</sub>. Each sample was analyzed in duplicate. Limits of detection for a 25 ml sample, including correction for blanks, were 2 pM COS, CS<sub>2</sub>, DMDS and isoprene, 15 pM DMS, 0.6 pM CH<sub>3</sub>I, 0.2 pM CH<sub>2</sub>ClI, 1.5 pM CH<sub>2</sub>Br<sub>2</sub> and CHBr<sub>3</sub>. For total DMSP (DMSP<sub>t</sub>) 35% HCl (10 mL per mL of sample) was added to unfiltered samples followed by storage at room temperature in the dark. To determine dissolved concentrations of DMSP (DMSP<sub>d</sub>), acrylate and DMSO, 15 ml sample aliquots were gravity filtered using precombusted 25 mm diameter Whatman glass-fiber (GF/F) filters into 20 ml scintillation vials. Filtrates were microwaved to boiling, bubbled with high-purity nitrogen gas to remove DMS, and acidified (Kinsey and Kieber, 2016). Back in our home lab, DMSP, and DMSP<sub>d</sub> were determined as evolved DMS by purge and trap gas chromatography with flame photometric detection, after alkaline hydrolysis. DMSO was determined as evolved DMS after reduction with TiCl<sub>3</sub>. Acrylate concentrations were determined using a precolumn derivatization HPLC method (Tyssebotn et al., 2017). The particulate forms of the three compounds (DMSP<sub>p</sub>, DMSO<sub>p</sub> and acrylate<sub>D</sub>) were determined by subtracting the dissolved from the total form. All analyses were run in duplicate.

# Sea surface temperature, chlorophyll *a*, nutrients, DOC, DON, POC, PON, and FDOM

The sea surface temperature (SST) was recorded on the boat with an SBE56 sensor (Sea-Bird Sci.) continuously flushed with pumped surface seawater.

For determination of chlorophyll *a* (Chla) concentrations, duplicate 250 mL aliquots of unfiltered seawater were taken from the sample carboys, filtered through 25 mm diameter GF/F filters and stored at -20°C until analysis. Chla extraction was performed in 90% acetone at 4°C for 24 h. The fluorescence of the extracts was measured with a calibrated Turner Designs fluorometer (model 10-AU-005 field fluorometer) equipped with an excitation and emission filters at 340-500 nm and above 665 nm, respectively.

For particulate organic carbon (POC) and particulate organic nitrogen (PON) analyses, 1.5 L seawater aliquots were taken from the carboys, filtered through precombusted (450°C for 4h) GF/F filters and stored frozen at -20°C until analysis. Filters for POC determination were decarbonated with acid vapor (Yamamuro and Kayanne, 1995). No replicates were analyzed. Carbon and nitrogen were determined with an elemental analyzer (Perkin-Elmer 2400 CHN). For the determination of total organic carbon (TOC) and total nitrogen (TN), unfiltered seawater aliquots (30 mL) were collected in acid-cleaned polycarbonate bottles and immediately stored at -20°C until analysis. Carbon and nitrogen were determined after inorganic C removal through acidification using a Shimadzu TOC VCSH instrument. Analytical quadruplicates were run. The equipment was calibrated with potassium hydrogen phthalate. High-purity laboratory water obtained from a MilliporeSigma Milli Q system (MilliQ water) was used as a blank and the reference material used was deep Sargasso Sea water (MRC Batch-15 Lot//11-15, measured TOC: 43.2 ± 1.1 μM, Dr. Dennis Hansell Laboratory, University of Miami, RSMAS). Dissolved organic carbon (DOC) concentrations were calculated by subtracting POC concentrations from TOC. Samples (10 mL) for inorganic nutrient determination were collected unfiltered and stored at -20°C until analysis. Concentrations of nitrate (NO<sub>3</sub>-), nitrite (NO<sub>2</sub>-), ammonia (NH<sub>4</sub>+), phosphate (PO<sub>4</sub><sup>3</sup>-) and silicate (SiO<sub>4</sub><sup>2-</sup>) were determined with an auto-analyzer (Bran Luebbe AA3) with spectrophotometric detection (Grasshoff, 1978). No replicates were analyzed. Dissolved organic nitrogen (DON) concentrations were calculated by subtracting inorganic nitrogen (nitrate, nitrite and ammonia) and PON concentrations from TN.

Characterization of fluorescent dissolved organic matter (FDOM) was performed with a Horiba Aqualog spectrofluorometer. Briefly, ca. 4 mL seawater aliquots were filtered through pre-combusted (450° C for 4 hours) GF/F filters. Fluorescence was recorded as square excitation-emission matrices in the 240-600 nm range. One to four analytical replicates were run. The intensity of peak T (hereafter referred to as FDOM-T), as defined by Coble (1996), was extracted as the fluorescence at excitation/emission wavelengths 275/340 nm using the *staRdom* package (Pucher et al., 2019). Fluorescence

intensity is presented in Raman Units (RU) after normalization to the Raman scatter measured in MilliQ water blanks (Lawaetz and Stedmon, 2009).

# Microorganism abundances and bacterial production

For the enumeration of heterotrophic prokaryotes (including bacteria and archaea) and pico- and nano-phytoplankton, 2-5 mL sample aliquots were fixed with glutaraldehyde (0.5%) and stored at  $-80^{\circ}\text{C}$  until analysis based on size and fluorescence on a flow cytometer capable of true volumetric absolute counting (CyFlow Cube 8, Sysmex Partec). Heterotrophic prokaryotes were stained with SYBRgreen I (~20  $\mu\text{M}$  final concentration) prior to quantification using green fluorescence. Prokaryotic (i.e., Synechococcus and Prochlorococcus) and eukaryotic pico- and nanophytoplankton were counted based on red and orange autofluorescence (Gasol and del Giorgio, 2000). No replicates were analyzed.

For bacterial biomass production estimates, 1 L of seawater was collected in acid cleaned amber bottles and stored at ambient temperature until further processing. The biomass production of the bacterial community was determined as described in Fadeev et al. (2023), based on the single-cell incorporation of Lhomopropargylglycine (HPG) into newly synthesized bacterial proteins (Samo et al., 2014). Briefly, seawater samples were amended with 50 µM HPG (final concentration of 20 nM) and incubated at in situ temperatures in the dark for 6 h. Afterwards, samples were fixed with formaldehyde (2-4% final concentration) at 4°C for at least 1 h in the dark and stored at -20°C until further processing. Prior to the microscopic analysis, the samples were stained with 2 µg mL-1 4',6-diamidino-2-phenylindole (DAPI) in Vectashield (Vector Laboratories, Newark, CA, USA). The cells were enumerated using a Zeiss Axio Imager M2 epifluorescence microscope (Carl Zeiss AG, Oberkochen, Germany) at 1250× magnification and the DAPI (Ex/Em = 358/461 nm) and the FITC (Ex/Em = 495/519 nm) filter sets. The bacterial abundance was calculated based on the average number of cells from at least 20 counting fields with 20-200 cells enumerated per counting field. At least 20 fields were counted for each filter slice using the Automated Cell Measuring and Enumeration Tool (ACMETool2, M. Zeder, Technobiology GmbH, Buchrain, Switzerland). The total abundance of biomass producing cells was determined as simultaneous signal of DAPI and FITC channels.

# Solar radiation

Global solar radiation (W/m<sup>2</sup>) data were provided by the meteorological station at the Gump Research Station (Washburn and Brooks, 2022), located 1.5 km and 5 km away from the sampling sites BR and OO, respectively.

# 16S/18S rRNA gene amplicon sequencing and processing

Single seawater aliquots (2 L, no replicates) for DNA collection were taken from the sampled carboys and filtered through 47 mm diameter polycarbonate filters of 0.2 µm pore size using a peristaltic pump. DNA filters were flash-frozen in liquid nitrogen and subsequently stored at -80°C. DNA extractions were performed using a standard phenol chloroform protocol (Massana et al., 1997) with a final step of purification using ultrafiltration in Amicon units (Millipore). Prokaryotic and eukaryotic diversity was determined by amplicon sequencing of the V4/V5 and V4 regions of the 16S and 18S rRNA genes, respectively, using the Illumina MiSeq platform and paired-end reads (2 × 250 bp). PCR amplifications were performed using (1) the prokaryotic universal primers 515F-Y (5'-GTGYCAGCMGCCGCGGTAA-3') and 926R (5'-CCGYCAATTYMTTTRAGTTT-3') (Parada et al., 2016) and (2) the eukaryotic universal primers V4F (5'-CCA GCA SCY GCG GTAATT CC-3') and V4R (5'-ACTTTC GTT CTT GAT YRR-3') (Balzano et al., 2015). All samples were sequenced at Research and Testing Laboratories (RTL, Lubbock, TX, USA) using the Illumina MiSeq platform ( $2 \times 250$  bp paired-end sequencing).

Illumina reads were processed as described in Masdeu-Navarro et al. (2022). Briefly, raw reads from both 16S and 18S rRNA gene sets were trimmed to remove amplification primers and spurious sequences using cutadapt v2.3 (Martin, 2011) and subsequently processed with DADA2 v1.4 (Callahan et al., 2016) to differentiate the 16S/18S rRNA gene amplicon sequence variants (ASVs) and to remove chimeras. ASVs were taxonomically assigned using the Ribosomal Database Project naïve Bayesian classifier (Wang et al., 2007), as implemented in DADA2, and an 80% minimum bootstrap confidence threshold using SILVA (v132; (Pruesse et al., 2007)) and PR2 (v4.11.1; (Guillou et al., 2013)) as reference databases for the 16S and 18S rRNA sets, respectively. Singletons and sequences affiliated to eukaryotes, organelles, or chloroplasts (for the 16S rRNA set) or to metazoans, Embryophyceae, Rhodophyta, Ulveophyceae or Phaeophyceae (for the 18S rRNA set) were removed.

To compare samples, ASV tables were randomly subsampled down to the minimum number of reads per sample for both rDNA sets (17,694 and 3,203 reads for the 16S and 18S rDNA sets, respectively) using the rarefy function in the vegan v2.5.7 package (Oksanen et al., 2021) in R v4.0.2 (R Development Core Team, 2021). The final ASV tables contained 2,018 prokaryotic ASVs and 1,473 protistan ASVs.

To gain insight into the diversity and temporal variation of the phototrophic eukaryotic assemblage (namely, autotrophs and mixotrophs), protistan ASVs were classified into four major functional groups on the basis of their taxonomic affiliation: autotrophs (obligate phototrophs), heterotrophs (mainly predators), mixotrophs, and parasites (including saprobes), based on previous works relative to the annotation into functional traits of protistan diversity (Genitsaris et al., 2015; 2016; Ramond et al., 2018; 2019; Minicante et al., 2019). ASV assigned at poor taxonomic resolution (e.g., unclassified Dinophyceae) or to a family/order of

organisms that include both autotrophs and heterotrophs (e.g., Gymnodiniaceae) were not attributed to any specific functional groups and were annotated as 'not determined (ND)". A detailed list of the classification for each protistan taxa is available in Supplementary Table S1.

# Data analysis

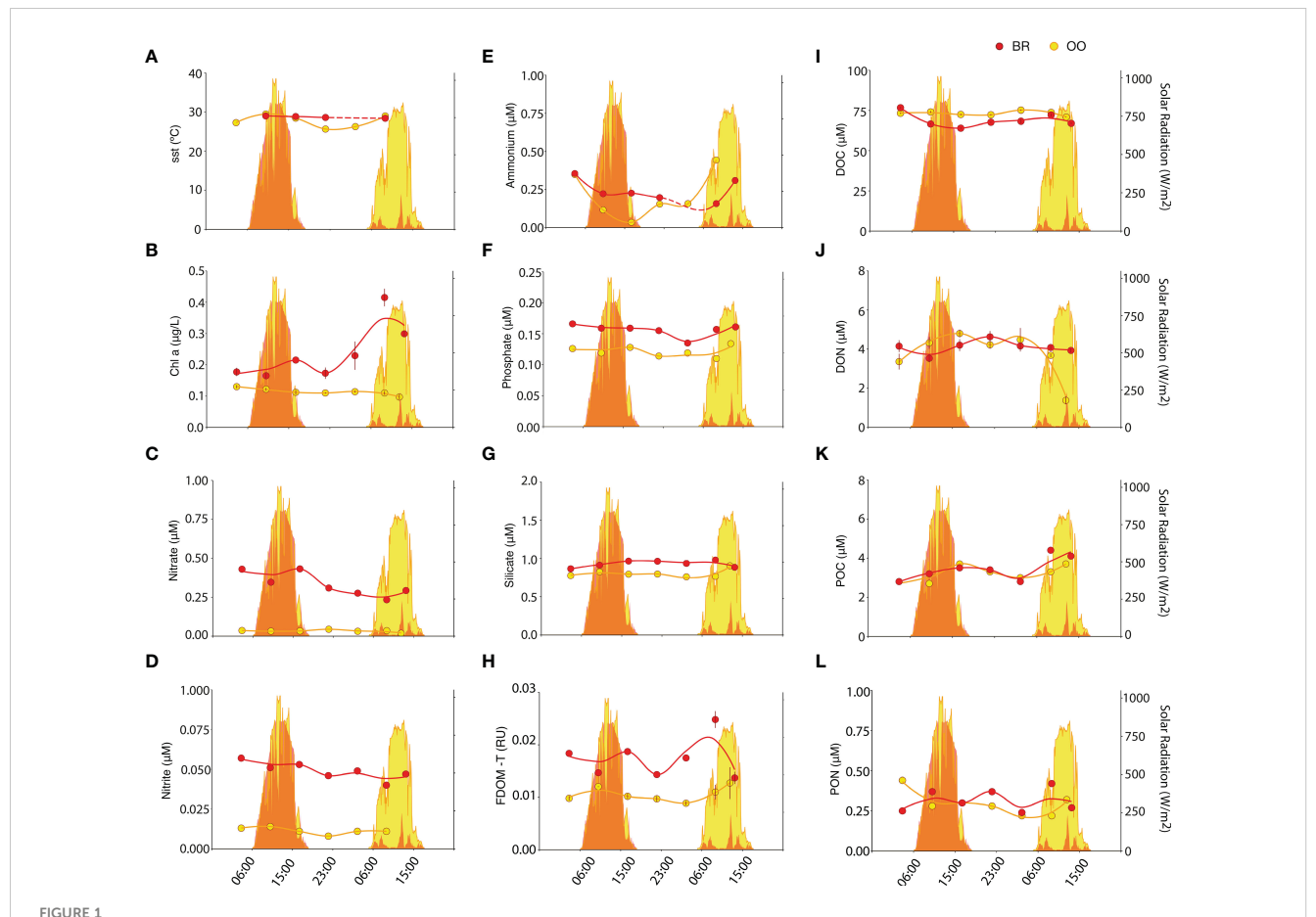
Statistical difference between the data series from both sampling sites (BR and OO) was evaluated with a non-parametric Kruskal-Wallis test. Spatial differences between the microbial community structure at each site obtained from the metabarcoding gene analysis were visualized using nonmetric multidimensional scaling (NMDS) based on Bray-Curtis distances and were obtained using the metaMDS function of the vegan R package. To investigate the relationships between VOCs and DMSPCs, and between these compounds and solar radiation, pairwise Spearman's correlations were computed with the ggcor v0.9–7 package in R (Houyun et al., 2020). Due to the short data series used (n=7), the threshold for correlation significance was set at p<0.1.

# Results and discussion

# Diel variation of environmental variables and microbial abundances

# Environmental variables

While solar radiation was similar at the two stations for the first respective sampling day, it was cloudy on the second sampling day at BR with substantially less solar radiation compared to that on the second sampling day at OO (Figure 1). The sea surface temperature (SST) showed a similar average at both sites (Kruskal-Wallis p>0.05) and stronger diel variation at OO (28.7  $\pm$  0.3°C in BR, 27.7  $\pm$  1.5°C in OO) (Figure 1A). This similarity despite the enormous difference in water column depth (2.5 m in BR, 1200 m in OO) highlights the strong connectivity of the two sampling sites. Indeed, the water flow across the reef is largely unidirectional: open ocean water enters the reef by wave action over the crest, flows across the back reef lagoon and exits the reef along the lagoon channel into Paopao Bay reef pass, where it flows out into the open ocean (Hench et al., 2008). Based on current speeds, the estimated residence time of seawater in the back reef lagoon is only a few hours, which is not sufficient to significantly warm it up. Nonetheless, the effect of weak tides and reef topography, where coral colonies can trap and recirculate waters in their wakes (Hench and Rosman, 2013), may complicate this speed-based estimate, resulting in a diel cycle of SST at BR that is less noticeable than that at OO (Figure 1A). In comparison to OO waters, the lagoon waters (BR) contained higher concentrations of Chla (0.25  $\pm$  0.09 vs 0.11 $\pm$  0.01  $\mu$ g/L; Kruskal-Wallis p<0.01), nitrate  $(0.33 \pm 0.08 \text{ vs } 0.03 \pm 0.01 \,\mu\text{M}; \text{Kruskal-Wallis p} < 0.01), \text{ nitrite } (0.049)$  $\pm$  0.005 vs 0.011  $\pm$  0.002  $\mu$ M; Kruskal-Wallis p<0.01), phosphate  $(0.16 \pm 0.01 \text{ vs } 0.12 \pm 0.01 \,\mu\text{M}; \text{Kruskal-Wallis p} < 0.01), \text{ silicate } (0.93)$  $\pm$  0.04 vs 0.80  $\pm$  0.05  $\mu$ M; Kruskal-Wallis p<0.01), and FDOM-T



Diel variation of environmental variables inside (back reef, BR; red) and outside (open ocean, OO; yellow) the coral reef. Dot plots depict the SST (A) and the concentrations of Chla (B), nitrate (C), nitrite (D), ammonium (E), phosphate (F), silicate (G), FDOM-T (H), DOC (I), DON (J), POC (K) and PON (L), measured over 34 h in BR (red) and OO (yellow). Trend lines were obtained by Loess regression. Colored areas in the background depict the total solar radiation at the two sites over the sampling period. Bars on dots in (B, H, I, J) depict the standard error of duplicate analyses.

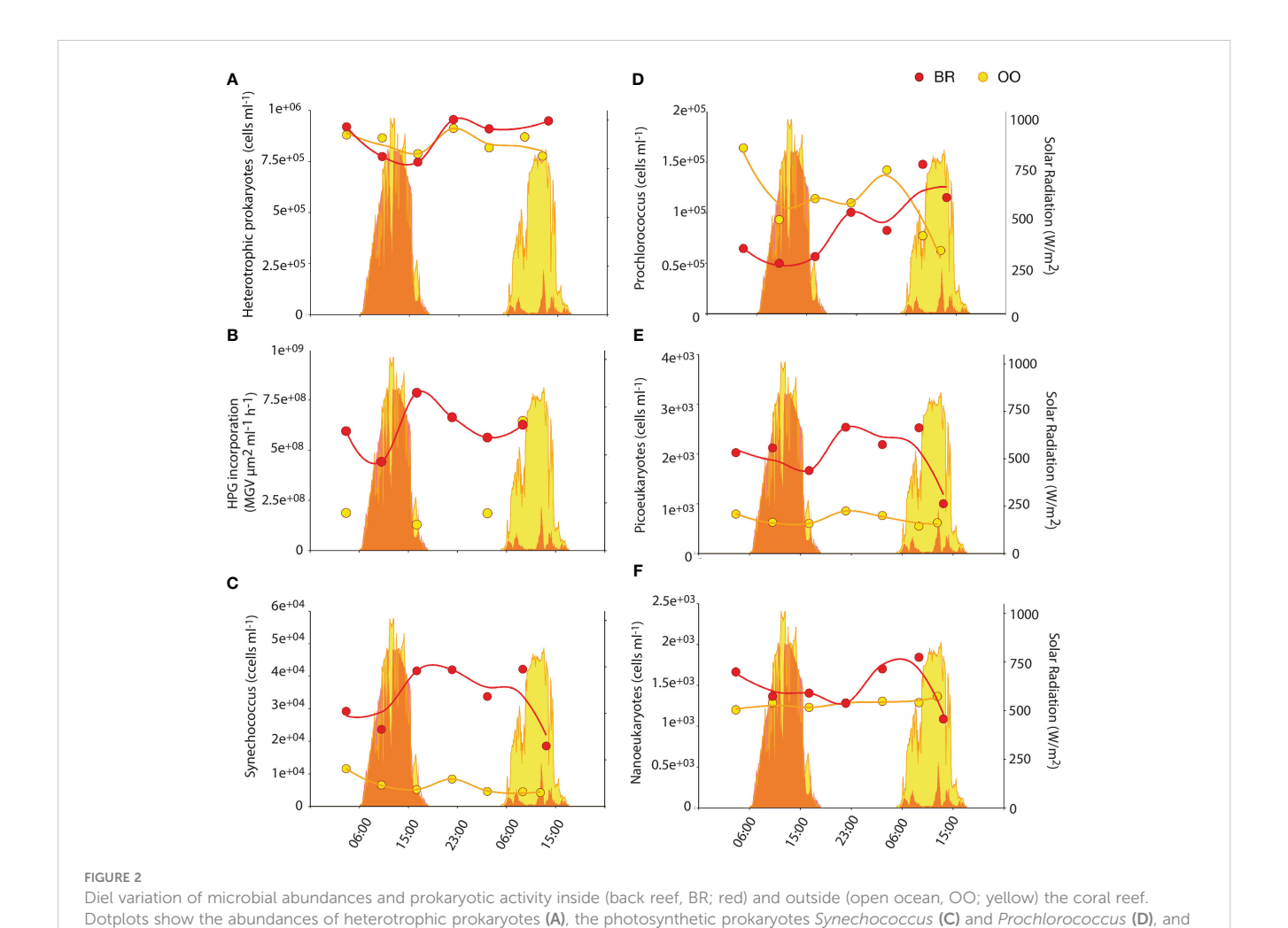
(0.017 ± 0.003 vs 0.011 ± 0.001 RU; Kruskal-Wallis p<0.01) (Figures 1B-H), suggesting there were additional reef or coastal (e.g., groundwater discharges; Haßler et al., 2019) sources for these variables. Conversely, DOC concentrations were lower at BR (68.9  $\pm$ 4.2 vs 73.1  $\pm$  1.4  $\mu$ M; Kruskal-Wallis p<0.05), and DON (4.1  $\pm$  0.3 vs  $4.1 \pm 0.5 \,\mu\text{M}$ ; Kruskal-Wallis p>0.05), POC (3.5 ± 0.6 vs 3.2 ± 0.4  $\mu\text{M}$ ; Kruskal-Wallis p>0.05) and PON (0.32  $\pm$  0.07 vs 0.29  $\pm$  0.07  $\mu$ M; Kruskal-Wallis p>0.05) concentrations were not consistently different from those at OO. Elevated concentrations of nitrate and depleted concentrations of DOC in the back reef lagoon relative to offshore surface waters have been documented and attributed to rapid rates of biological activity by both planktonic and benthic organisms (Leichter et al., 2013). The presence of additional sources of suspended microalgal biomass in the reef, such as released epiphytic, benthic, and coral associated microalgae, may explain the higher Chla in BR. Furthermore, the elevated concentration of silicate can be regarded as a biogeochemical marker of coastal influence to the lagoon.

POC was the only biogeochemical variable that showed a noticeable diel pattern at both sampling sites (Figure 1K). It accumulated over the day and decreased overnight at BR and OO, which may depict the diel cycle of planktonic photosynthesis

(POC production) and mortality (POC loss), similar at both sites. DOC (Figure 1J) generally followed the opposite pattern, lower during the day and increasing during the night. This would indicate a dynamic partitioning between the two organic carbon pools over the diel cycle. At OO, FDOM-T, which is a signature of freshly produced, labile and protein-rich DOM (Coble, 1996), showed a clear diel pattern that paralleled that of POC, with a daytime increase, presumably from photosynthesis-driven release of DOM, and nighttime decrease, indicative of respiration-driven net consumption (Figure 1H). At BR, FDOM-T concentrations were higher than at OO but did not exhibit diel pattern, likely because of multiple sources besides plankton, including sediments, seaweeds, corals and groundwater discharges.

# Microbial abundances

Heterotrophic prokaryotic abundances were very similar in BR and OO (9.1E5  $\pm$  1.3E5 vs 8.4E5  $\pm$  0.5E5 cells/mL; Kruskal-Wallis p>0.05) and so were their diel patterns, with increased abundances in the early evening (Figure 2A). In contrast, heterotrophic prokaryotic production (as revealed by HPG incorporation) was ~3 times higher at BR compared to that at OO (Figure 2B). The release of fresh and labile DOC by the coral



photosynthetic picoeukaryotes (E) and nanoeukaryotes (F) over 36 h at BR (red) and OO (yellow). Also shown (B) is the heterotrophic prokaryotic activity measured as L-homopropargylglycine (HPG) incorporation. Trend lines were obtained by Loess regression. Colored areas in the background

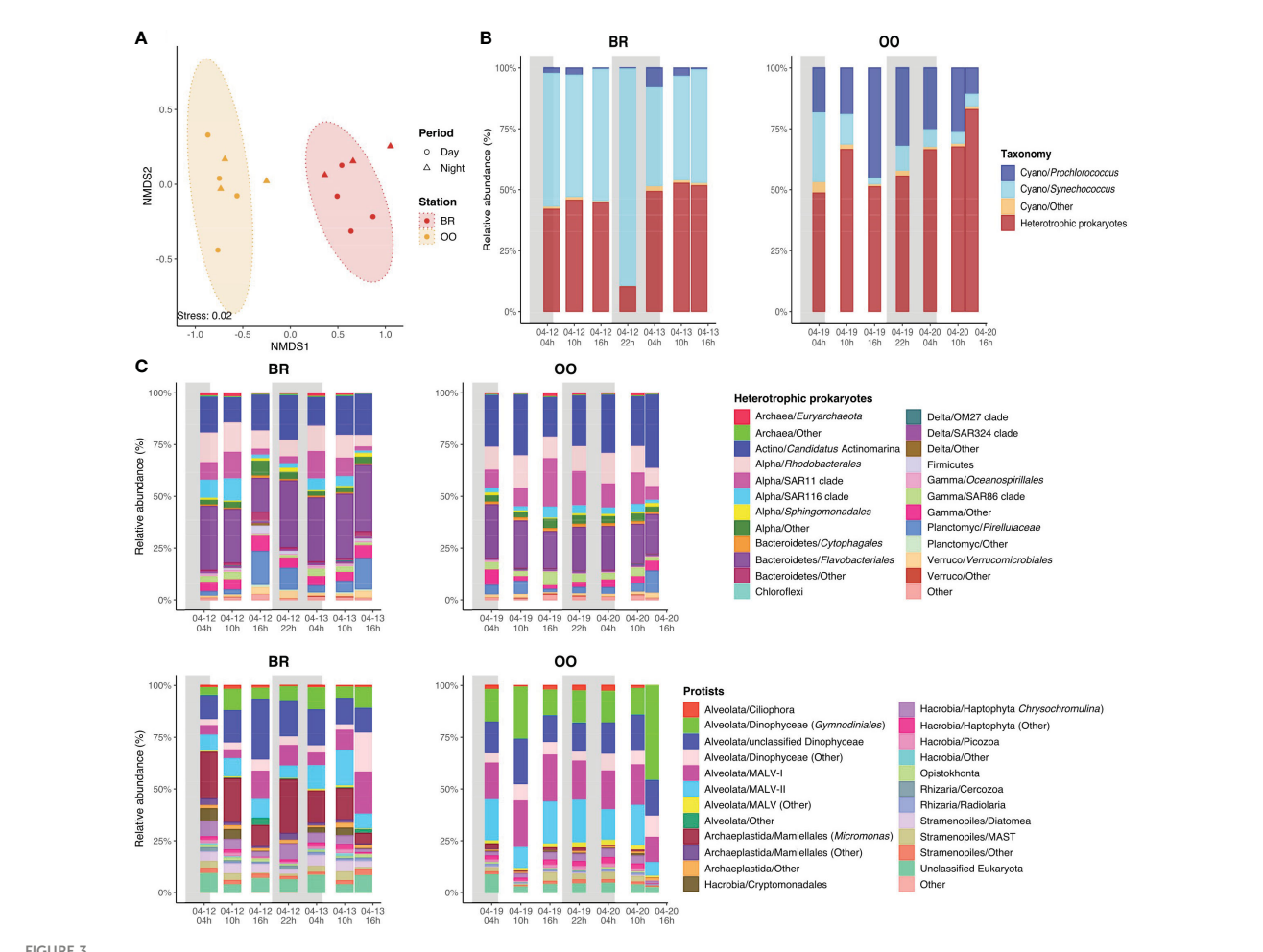
symbionts Symbiodiniaceae and seaweeds inside the reef may trigger higher heterotrophic prokaryotic activity even at the expense of imported semi-recalcitrant DOC from the open ocean (Nelson et al., 2011).

depict the total solar radiation at the two sites over the sampling period

In contrast to what was observed with heterotrophic microbes, lagoon waters (BR) harbored higher abundances of phytoplankton, especially the cyanobacterium Synechococcus and the picoeukaryotes that were, on average, 5 and 3.3 times more abundant (Kruskal-Wallis p<0.01), respectively, at BR than at OO (Figures 2C, E). This was not significant (Kruskal-Wallis p>0.05) for the nanoeukaryotic phytoplankton (Figure 2F) and opposite for Prochlorococcus during most of the time series (Figure 2D), as already documented for a nearby reef (Payet et al., 2014). Phototrophic microbes in BR did not exhibit diel synchrony; Synechococcus doubled during the day, picoeukaryotes increased by 1.5 in early night, and nanoeukaryotes increased by 1.3 in late night. Prochlorococcus appeared to follow the same diel pattern as picoeukaryotes, but the large increase on the second day may be caused by increased Chla fluorescence per cell due to much lower solar radiation, resulting in better detection in the flow cytometer (Sommaruga et al., 2005).

# Diel variation of the microbial community composition and diversity

A total of 2,018 prokaryotic and 1,473 protistan ASVs were retrieved over the diel cycles at BR and OO (Figure S1A). Rarefaction curves for both the 16S and 18S rRNA datasets and sampling time points approached a plateau in most cases, indicating that a substantial portion of microbial diversity was captured in each sample (Figure S1B). Clustering of the microbial community by their Bray-Curtis dissimilarities using the combined 16S and 18S ASV datasets revealed a clear separation of the two sampling sites (Figure 3A). BR and OO shared ~25% of the total prokaryotic ASVs and ~40% of the total eukaryotic ASVs (Figure S1A). Furthermore, 70% of the prokaryotic ASVs from BR were specific to the site. In BR and OO, an average of ~57% and 37% of the prokaryotic ASVs corresponded to cyanobacterial taxa, respectively (Figure 3B). Among the cyanobacteria, the most abundant genera were Synechococcus, (80-99% predominant at BR) and Prochlorococcus (35-92% at OO), confirming the results of flow cytometry (Figures 2, 3B). The main heterotrophic prokaryotic components in BR were from the order Flavobacteriales (Bacteroidetes),



Characteristics of the microbial communities present over the diel cycles (back reef, BR) and outside (open ocean, OO) the coral reef. (A) The similarity of the microbial community structure (prokaryotes and protists together) assessed by non-metric multidimensional scaling analysis (NMDS) biplot based on Bray-Curtis dissimilarities with colored ellipses indicating the two groupings with a confidence level of 95%. (B) Diel variation of the main cyanobacterial genera in the prokaryotic assemblage at BR and OO. (C) Diel variation of the taxonomic composition of the heterotrophic prokaryotes and phototrophic eukaryotes (protists) in BR and OO. Shaded boxes in (B, C) indicate the night period.

representing 16-32% of the total ASVs, and the coral-reef characteristic bacteria Candidatus *Actinomarina* (Apprill et al., 2016), accounting for 13-22% of the prokaryotic ASVs (Figure 3C). To a lesser extent, sequences of alphaproteobacterial clades (such as *Rhodobacteriales*, SAR11 and SAR116) and *Planctomycetes* (*Pirellulaceae*) together represented 24-40% of the total prokaryotic diversity. Essentially the same main taxonomic groups were retrieved in OO despite the low share of ASVs with BR (Figure 3C). Yet, a change in the dominance was observed, with Candidatus *Actinomarina* being the most abundant (20-36%), followed by *Flavobacteriales* (19-26%), SAR11 (7-23%) and *Rhodobacteriales* (9-16%).

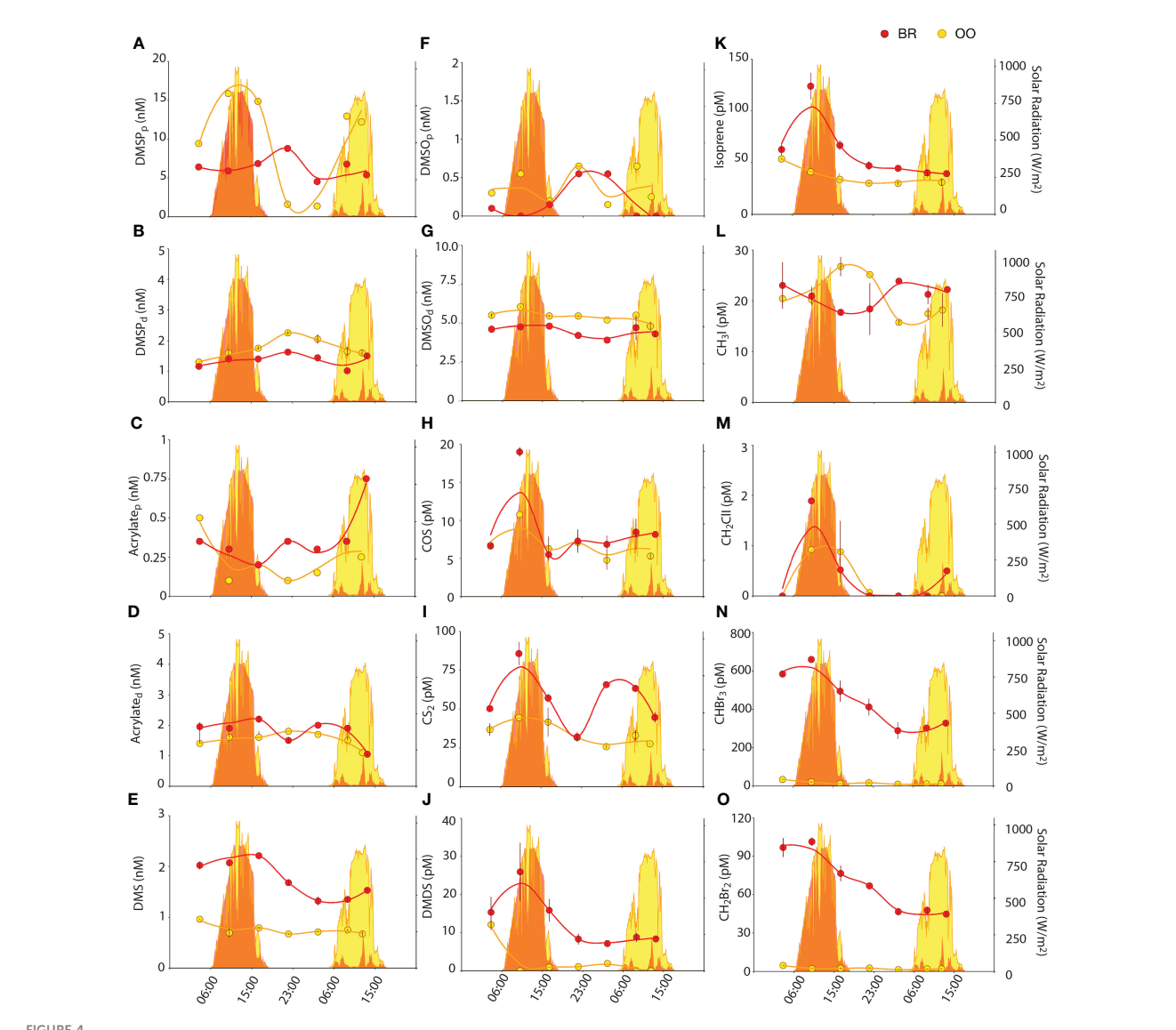
Regarding the eukaryotes, the relative abundance and diel variation of the protistan assemblages are shown in Supplementary Table S1. The phototrophic eukaryotic assemblages (i.e., autotrophs and mixotrophs) were similar at both sites, with abundant sequences affiliated to dinoflagellates and haptophytes (Figure 3D). The largest difference between the two sites was the presence of the green algae *Mamiellales* (specifically, *Micromonas* sp.) at BR, where they represented up to

53% of the eukaryotic phytoplankton sequences, and their virtual absence at OO (<2.5%). Other groups present at BR and absent at OO were *Cryptomonadales* and diatoms.

The low dispersion of the data clouds in the NMDS ordination (Figure 3A) suggests that the microbial diversity was relatively stable over time at both sites, which was confirmed when examining the taxonomic compositions (Figures 3B-D). In conclusion, our metabarcoding analysis confirmed the presence of two distinct bacterioplankton and phytoplankton assemblages at BR and OO, each with a rather stable composition over the diel cycle.

# Diel variation of DMSPC concentrations inside and outside the reef

For the non-volatile DMSPCs (DMSP, acrylate, DMSO), there were no remarkable differences in the partitioning between the particulate and dissolved pools at the two sampling sites (Figures 4A–D, F, G). DMSP was 5–19% dissolved at BR, and 8–25% at OO. Acrylate was 58–92% dissolved at BR, and 74–95% at



Diel variations of particulate and dissolved DMSPC concentrations, and VOC concentrations, (back reef, BR; red) and outside (open ocean, OO; yellow) the coral reef. Dot plots show the concentrations of DMSPCs (DMSP $_p$  (A), DMSP $_d$  (B), acrylate $_t$  (C), acrylate $_d$  (D), DMS (E), DMSO $_t$  (F), DMSO $_d$  (G), DMDS (J)) and VOCs (COS (H), CS $_2$  (I), Isoprene (K), CH $_3$ I (L), CH $_2$ CII (M), CH $_2$ Br $_2$  (O)) over 36 h at BR (red) and OO (yellow). Bars on dots indicate the standard error of duplicate analyses. Zero values in the DMDS and CH $_2$ CII plots indicate below detection limit. Trend lines were obtained by Loess regression. Colored areas in the background depict the total solar radiation at the two sites over the sampling period.

OO. DMSO was 88–100% dissolved at BR, and 89-97% at OO. The particulate concentrations of the three compounds were similar at the two sites (Kruskal-Wallis p>0.05), which could be coincidental or indicative of rapid connectivity through the water flow (Hench et al., 2008; Leichter et al., 2013). In contrast, the dissolved concentrations of DMSP and DMSO were slightly higher at OO (Kruskal-Wallis p<0.05), indicative of higher microbial DMSP<sub>d</sub> consumption at BR (Xue et al., 2022) and higher photochemical DMSO<sub>d</sub> production at OO (see below). The concentrations of the volatile DMSPCs, namely DMS and DMDS, were higher at BR (Kruskal-Wallis p<0.01) by factors of 1.3-3 and 1.2->20, respectively. Note that we interpret the occurrence of DMDS in the Mo'orean seawater chromatograms as a non-quantitative reflection of the presence of methanethiol (MeSH), since the high temperatures and activated carbon of our purge and trap system are

expected to partly oxidize MeSH to DMDS during the analysis (Cheng et al., 2007). Indeed, DMDS concentrations in OO (0-10 pM) were much lower than the few existing measurements of MeSH in low-Chla tropical waters of the Atlantic (100-300 pM; Kettle et al., 2001). DMS concentrations in OO (0.6-1 nM) were near the lower end of previous measurements in the tropical oligotrophic oceans (1-5 nM; Dani and Loreto, 2017). The higher concentrations of both compounds in BR could be due to non-planktonic sources of DMS and MeSH within the reef, such as DMSP degradation in coral holobionts (Masdeu-Navarro et al., 2022), seaweeds (Burdett et al., 2013), and sediments (Deschaseaux et al., 2019).

Non-volatile DMSPCs exhibited diel patterns, however these patterns were different between compounds and sites. At OO, particulate DMSP (DMSP<sub>p</sub>) increased during the day and decreased at night, following solar radiation (Figure 4A). Even

though DMSP<sub>p</sub> is known to be associated with phytoplankton (Stefels et al., 2007 and references therein), its diel pattern did not follow size and fluorescence-based phytoplankton abundances (Figure 2) or Chla concentrations (Figure 1B). The closest pattern of a biogeochemical variable was that of POC (Figure 1K); however, the DMSP<sub>p</sub>/POC ratio increased during the day, somehow amplifying the diel cycle observed with POC (Figure 5A). This suggests that intracellular DMSP in the open ocean varies partly with phytoplankton biomass and partly with photophysiology, so that DMSP biosynthesis increases with light (Simó et al., 2002). In the tropical Atlantic, Archer et al. (2018) measured higher rates (d-1) of DMSP synthesis than rates of carbon fixation into POC at all irradiances, an expected result since a substantial proportion of POC is detrital and heterotrophic biomass, while most DMSP is contained in phytoplankton. This may explain the amplitude of the DMSP<sub>p</sub>/POC ratio over the diel cycle at OO. Another example of a molecule that varies with both biomass and photophysiology is Chla, whose cellular concentration varies over diel cycles (Owens et al., 1980). At OO, Chla varied with an opposite pattern to that of POC, so that the Chla/POC ratio increased at night and decreased during the day (Figure 5B). At BR, the DMSP<sub>p</sub> diel trend was virtually opposite to that at OO, with a nighttime peak, even though the POC diel pattern was the same at both sites (Figure 4A).

A Spearman's correlation analysis (Figure 6) confirmed that DMSP<sub>p</sub> covaried significantly and positively with solar radiation at OO but not at BR. This discrepancy might be because, in our Mo'orean reef lagoonal waters, DMSP<sub>p</sub> sources not only include plankton but also corals, seaweeds and sediment debris. In support of this, the 16S rRNA metabarcoding analysis (Figure 3C) revealed abundant sequences of Planctomycetes and Verrucomicrobia, typically associated with macroalgae and sediments. However, DMSP<sub>p</sub> concentrations (1.4-15.9 nM) were lower at BR over most of the diel cycle, even though Chla concentrations and phytoplankton abundances were higher, and the aforementioned contribution from debris was expected; therefore, ecophysiological explanations are to be invoked. First, the relative abundances of protistan taxonomic groups, as described by metabarcoding with the 18S rRNA gene (Figure 3C), depicted higher abundances of haptophytes and dinoflagellates at OO, especially Gymnodiniales and Prorocentrales that are reported to contain moderate to very high cellular DMSP concentrations (Keller et al., 1989) and contribute to high DMSPC concentrations in the surface ocean (Saint-Macary et al., 2023). Indeed, microscopy counts revealed that the biomasses of coccolithophores and dinoflagellates, two groups that are prolific DMSP producers, were higher at OO than at BR by a factor of 4 (Masdeu-Navarro et al., unpublished). Second, back reef waters contained 5 to 10-fold higher concentrations of nitrate (Figure 1C), likely due to microbial nitrification exacerbated by microbes associated with sediments and benthic filter-feeders (Scheffers et al., 2004; O'Neil and Capone, 2008); Groundwater inputs cannot be rule out either. Relieving acute nitrate limitation has been reported to decrease phytoplankton intracellular DMSP<sub>p</sub> concentrations (Bucciarelli and Sunda, 2003).

DMSO<sub>p</sub> concentrations were quite low (0.1-0.6 nM) at both sites. This was unexpected, since a previous meta-analysis had shown that the intracellular DMSO pool relative to DMSP typically increases towards the high seawater temperatures observed during our study (Simó and Vila-Costa, 2006). Furthermore, DMSO<sub>p</sub> exhibited a diel peak around midnight (Figure 4F). The hypothesis of an antioxidant role for DMSP under high irradiances (Sunda et al., 2002) would imply higher intracellular DMSO production rates during the day, but whether this should result in intracellular accumulation is unknown. Correlation analysis (Figure 6) did not show covariation of DMSO<sub>p</sub> with any potentially regulatory variables, and too little is still known about this cellular component to provide a unequivocable explanation for the low levels and daily pattern of DMSO<sub>p</sub> observed in Mo'orean waters. Particulate acrylate (acrylate<sub>p</sub>) followed diel patterns (Figure 4C) that somewhat paralleled those of DMSP<sub>p</sub> at both sites, which was expected since the latter is precursor of acrylate through intracellular cleavage (Kinsey and Kieber, 2016). Dissolved concentrations of DMSP (DMSP<sub>d</sub>) and acrylate (acrylate<sub>d</sub>) varied opposite to their particulate pools in OO, with a maximum at night likely attributed to intracellular release through grazing-driven mortality (Figures 4B, D). At BR, acrylate<sub>d</sub> and DMSO<sub>d</sub> were also opposite to their particulate pools, but DMSP<sub>d</sub> paralleled DMSP<sub>p</sub>. We note that DMSO can also be produced through cleavage of the recentlydiscovered intracellular component DMSOP (Thume et al., 2018), which unfortunately was not measured. A variety of microorganisms, including the microalgae haptophytes and dinoflagellates and the bacteria SAR11 and Rhodobacteriales, are

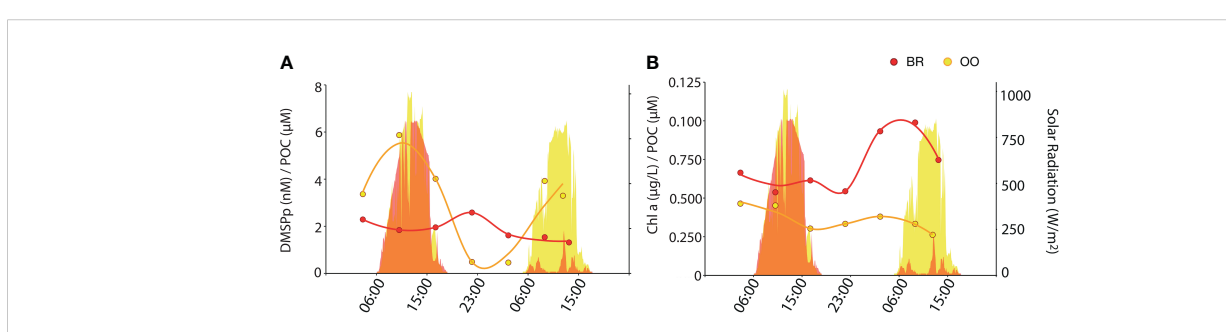
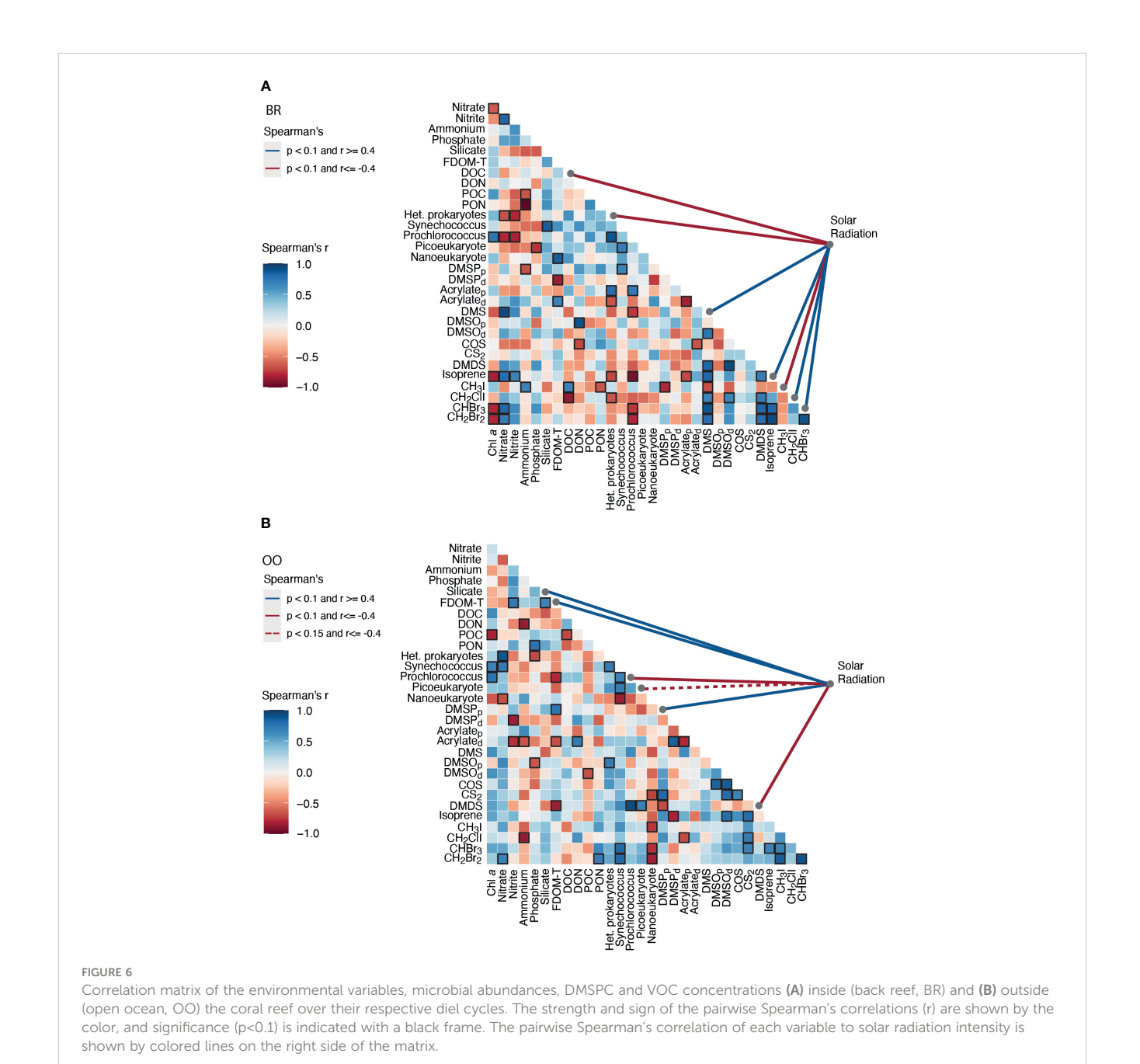


FIGURE 5
Diel variation of DMSP<sub>p</sub> and Chla concentrations normalized to the POC concentration (back reef, BR; red) and outside (open ocean, OO; yellow) the coral reef. Dotplots show the values of the DMSP<sub>p</sub>/POC (A) and Chla/POC (B) ratio over 36 h at BR (red) and OO (yellow). Trend lines were obtained by Loess regression. Colored areas in the background depict the total solar radiation at the two sites over the sampling period.



capable of cleaving DMSOP to DMSO and acrylate using the same lyases for DMSP (Carrión et al., 2023).

As for the volatile DMSPCs, the most striking feature was the pronounced diel patterns of DMS and DMDS concentrations at BR (Figures 4E, J). Both compounds decreased at night and increased during the day, with a comparatively lesser increase on the second, cloudy day. This resulted in a significant positive correlation of DMS to solar radiation (Figure 6A). This lends support to the hypothesis that DMS is produced by and released from planktonic and benthic microalgal cells (including coral-associated Symbiodiniaceae) in response to high irradiance or due to its antioxidant properties (Sunda et al., 2002; Slezak et al., 2007; Galí et al., 2013a, Galí et al., 2013b; Lawson et al., 2021; Masdeu-Navarro et al., 2022). Alternatively, the energy of midday incident radiation can easily exceed the photosynthetic electron transport capacity,

conditions under which DMSP can be released, as such or upon transformation into DMS, as a strategy to dissipate excess energy (Stefels, 2000; Kinsey et al., 2023). The hypotheses of oxidative stress and excess energy dissipation are not mutually exclusive, and support to the latter is given by the fact that DMDS (hence MeSH) behaved the same as DMS (positive Spearman's correlation, Figure 6A), suggesting DMSP release by phytoplankton as well as corals (Masdeu-Navarro et al., 2022) and rapid bacterial degradation to DMS, acrylate<sub>d</sub> and MeSH. Note that the prokaryotic assemblages at the two sites (Figure 3C) contained abundant taxa within *Rhodobacteriales*, SAR11, SAR116 and gamma-proteobacteria that are known to harbor *ddd*- genes for DMSP cleavage into DMS and acrylate, as well as taxa within SAR11, *Rhodobacteriales*, SAR116 and other alpha-proteobacteria harboring the *dmdA* gene that eventually leads to MeSH production

(González et al., 2019; Tang and Liu, 2023). Acrylate<sub>d</sub>, in turn, would be quickly consumed by bacteria (Xue et al., 2022), and MeSH would be both biologically consumed and (photo)chemically oxidized to DMDS. In line with this, bacterial activity at BR was higher during the day (Figure 2B) and so were bacterial DMSP<sub>d</sub> and acrylate<sub>d</sub> consumption rates (Xue et al., 2022).

In reef lagoonal waters of the Great Barrier Reef, Broadbent and Jones (2006) reported diurnal increases in DMS and DMSP<sub>p</sub> concentrations, which they attributed to a physiological response of coral holobionts to increased light and temperature, including the use of these compounds by endosymbiotic Symbiodiniaceae to scavenge reactive oxygen species (Jones and King, 2015), and the diurnal expulsion of endosymbionts by the coral. However, shortterm variation of DMSPCs was also largely affected by tides (Broadbent and Jones, 2006; Jones et al., 2018). Higher DMS concentrations coincided with low tides, and the greatest effect occurred when corals were exposed to air at very low tides. DMS production was further exacerbated if a low tide coincided with rainfall. The effect of tides on coral DMS production is explained by the stress that low tides impose on corals, more so if corals are exposed to air. In our Mo'orean reef, though, conditions were very different: tides were semi-daily (low tide around 6:00 and 18:00) and weak, with an amplitude of ca. 30 cm, and corals were not exposed to air. Our results (Figures 4E, 6A) suggest that solar radiation was the main driver of diel DMS variability in the reef.

The daytime increase in DMS was not observed at OO, probably because DMS was released at lower rates and concentrations were capped by DMS photolysis (Galí and Simó, 2015). In agreement with this interpretation, the concentrations of DMSO<sub>d</sub>, a major product of DMS photooxidation (Hopkins et al., 2023), were higher at OO and sightly increased in the morning (Figure 4G).

# Diel variation of VOC concentrations inside and outside the reef

# Other volatile sulfur compounds (COS and CS<sub>2</sub>)

COS concentrations ranged 5-15 pM, at the lower end of previous observations in tropical waters (3-134 pM; Lennartz et al., 2017), and were similar at the two sampling sites, only slightly higher at BR (Kruskal-Wallis p>0.05; Figure 4H). COS increased in the morning, and faster at BR and on the first (sunny) day. This is consistent with COS photochemical production from the photolysis of chromophoric dissolved organic matter (Uher and Andreae, 1997). A positive correlation of COS to DMSO<sub>d</sub> at OO (Figure 6) pointed to a common origin of these two compounds through photochemical reactions in the presence of dissolved organic matter. Modiri Gharehveran and Shah (2018) suggested that COS may partly be formed through DMS photooxidation, like DMSO<sub>d</sub>. Note, however, that these authors used DMS concentrations as high as 14 µM to show conversion into COS; therefore, for such a process to be a significant source of COS in marine environments (relative to UV photoproduction from dissolved organic matter), it should occur in DMS-enriched layers around cells and aggregates. In our diel study, the maximum COS concentration was followed by net consumption in the afternoon at both sampling sites (Figure 4H). Besides being ventilated to the atmosphere, COS is removed mainly by abiotic hydrolysis, which is accelerated in warm waters (Lennartz et al., 2020).

CS<sub>2</sub> concentrations varied from 25 to 75 pM, within the range of measurements in the tropical oceans (0.2-155 pM; Lennartz et al., 2017), and were higher at BR compared to OO (Kruskal-Wallis p<0.05). At the sea surface, this compound is also produced photochemically from chromophoric dissolved organic matter (Xie et al., 1998) as well as biologically by phytoplankton (Xie et al., 1999). Removal processes other than ventilation to the atmosphere are unknown and thought to be inefficient (Lennartz et al., 2020), yet a first order sink process had to be invoked to fit a model to CS<sub>2</sub> observations in the Atlantic Ocean (Kettle, 2000). Consumption by aerobic bacteria has long been known (Kelly and Smith, 1990) but its relevance in seawaters has yet to be proven. As a result of the net balance between sources and sinks, CS2 concentrations depicted a diel pattern at OO, with a daytime peak (Figure 4I). At BR, CS<sub>2</sub> concentrations were higher than in the open ocean, consistent with higher water-column integrated irradiances because of shallower mixing, and higher levels of fresh organic matter. In contrast to OO, there was no identifiable diel pattern of CS<sub>2</sub> at BR, which suggests a large contribution from a sedimentary bacterial source (Kim and Andreae, 1992).

### Isoprene

Isoprene concentrations were 30-50 pM in offshore waters, within the range observed in the tropical oceans (20-90 pM; Dani and Loreto, 2017). Higher concentrations occurred at BR (40-120 pM) (Kruskal-Wallis p<0.05; Figure 4K). A diel variation driven by sunlight was most obvious at BR, to the extent that isoprene correlated with solar radiation (Figure 6A). A daytime peak for seawater isoprene has already been reported (Matsunaga et al., 2002; Wu et al., 2021) and suggested to be linked to phytoplankton photosynthetic activity and oxidative stress (Dawson et al., 2021). Endosymbiotic Symbiodiniaceae also produce isoprene in coral holobionts (Exton et al., 2015), especially under environmental stress (Swan et al., 2016; Dawson et al., 2021). Another source is the sediment microphytobenthos, which also produce more isoprene during the day (Hrebien et al., 2020). Altogether, these sources may explain the increase of isoprene concentration in the morning at BR (Figure 4K). Microbial and chemical (oxidation) consumption observed in these same waters (Simó et al., 2022) would explain the afternoon decrease. Note that major bacterial consumers of isoprene are the Actinobacteria (Acuña Alvarez et al., 2009; Dawson et al., 2021), which were abundant at both sampling sites. Additional loss by reaction with H<sub>2</sub>O<sub>2</sub> and bromoperoxidases (Simó et al., 2022) would have been faster at BR due to the presence of dense populations of seaweeds (Masdeu-Navarro et al., 2022).

### **lodomethanes**

The two iodomethanes detected and quantified were  $\mathrm{CH_{3}I}$  and  $\mathrm{CH_{2}CII}$ .  $\mathrm{CH_{3}I}$  concentrations ranged 16-28 pM, at the upper end of published measurements in the tropical Pacific (0.6-19 pM; Fuhlbrügge et al., 2016). Concentrations were not significantly different at the two sampling sites (Kruskal-Wallis p>0.05), but

the diel patterns were opposite (Figure 4L). At OO, CH<sub>3</sub>I increased over the course of the day and decreased overnight, so that the maximum was at dusk and the minimum at dawn. Previous work suggested a photochemical source (Happell and Wallace, 1996; Richter and Wallace, 2004) that could explain this pattern. CH<sub>3</sub>I is also produced in phytoplankton cultures (diatoms, phototrophic picoeukaryotes, Prochlorococcus and Synechococcus; Yokouchi et al., 2014); furthermore, iodide methylation by both prokaryotes and eukaryotes has been seen to occur in the marine environment (Amachi, 2008). However, the rapid consumption overnight in the open ocean is puzzling because chemical destruction is esteemed too slow (lifetime of 8 weeks; Jones and Carpenter, 2007) to have a measurable, short-term impact on CH<sub>3</sub>I concentrations. At BR, CH<sub>3</sub>I concentrations decreased during the day and increased overnight, so that the maximum was at dawn and the minimum was at dusk (Figure 4L). This was opposite to the diel pattern observed at OO and indicates a yet unknown sunlightdependent or circadian loss. Therefore, the role of each of the diverse reef components in CH<sub>3</sub>I cycling is yet to be resolved.

CH<sub>2</sub>CII concentrations ranged between undetectable and 2 pM, at the lower end of observations in non-upwelling tropical waters (<2-6 pM; Jones et al., 2010). Concentrations were comparable between sampling sites (Kruskal-Wallis p>0.05), and diel patterns followed the sunlight cycle (Figure 4M). At BR, this was reflected by a significant positive correlation of CH<sub>2</sub>CII to solar radiation (Figure 6A). CH<sub>2</sub>CII is mainly produced by light-enhanced halide substitution from CH<sub>2</sub>I<sub>2</sub> (Martino et al., 2006), and this is the reason why CH<sub>2</sub>I<sub>2</sub> concentrations anticorrelate with solar radiation and decrease during the day in the surface ocean (Hepach et al., 2015). CH<sub>2</sub>I<sub>2</sub> is produced by phytoplankton and especially by tropical seaweeds including the genus *Turbinaria* (Keng et al., 2021). Indeed, we observed CH<sub>2</sub>I<sub>2</sub> in our study, yet it was detectable only in a few samples and could not be reliably quantified.

### **Bromomethanes**

Concentrations of CHBr<sub>3</sub> and CH<sub>2</sub>Br<sub>2</sub> at the open ocean site OO ranged 10-34 pM and 1-5 pM, respectively, within the lower range of previous measurements in the tropical Pacific (3-137 pM CHBr<sub>3</sub> and 2-22 pM CH<sub>2</sub>Br<sub>2</sub>; Fuhlbrügge et al., 2016). They showed no identifiable diel pattern (Figures 4N, O). Concentrations were more than an order of magnitude higher (Kruskal-Wallis p<0.01) in the back reef waters of BR (289-659 pM CHBr<sub>3</sub> and 45-101 pM CH<sub>2</sub>Br<sub>2</sub>), with higher concentrations during the day, particularly on the first sunny day. This resulted in significant positive correlation of CHBr<sub>3</sub> to solar radiation (Figure 6A). The two compounds were strongly positively correlated at both sites, a common feature in tropical waters (Hepach et al., 2015), with CHBr<sub>3</sub>:CH<sub>2</sub>Br<sub>2</sub> ratios around 7 (OO) and 6.5 (BR). Marine bromomethanes, especially bromoform (CHBr<sub>3</sub>), have their origin in the reaction of bromoperoxidases (BrPO) with H<sub>2</sub>O<sub>2</sub> in the presence of organic matter (Manley, 2002). Phytoplankton and macroalgae use BrPO to scavenge harmful levels of peroxide (Carpenter et al., 2012). Large amounts of CHBr3 are produced by seaweeds in response to exposure to sunlight (Keng et al., 2013), as a mechanism to cope with oxidative stress (Manley and Barbero, 2001). This explains why

bromomethane concentrations were so much higher at BR than at OO, given the spread of seaweed coverage across the reef crest and back reef, especially of the brown alga *Turbinaria ornata* (Masdeu-Navarro et al., 2022). Seaweed production also explains the strong diel cycle observed at BR, which was already reported for macroalgal-colonized coastal pools in early studies (Ekdahl et al., 1998). At OO, instead, bromomethanes were positively correlated to *Synechococcus*, a cyanobacterial taxon known to harbor BrPO (Johnson et al., 2011).

CHBr<sub>3</sub> is efficiently transformed to CH<sub>2</sub>Br<sub>2</sub> by bacteria (Kataoka et al., 2019), including *Rhodobacterales* (Ichikawa et al., 2015), a taxonomic group that was abundant at both sampling sites (Figure 3C). Sinks for bromomethanes, besides ventilation, are photolysis (Carpenter and Liss, 2000), halide substitution (Quack and Wallace, 2003), and consumption by nitrifying bacteria (Wahman et al., 2006). Based on our dataset, we cannot say which factors controlled the dramatic consumption of bromomethanes at BR, particularly at night.

# Summary: what controls the diel variation of DMSPC and VOC concentrations in the open ocean and in the reef lagoon?

Despite being in the same climatic zone, the two sampling sites were in markedly different ecosystems. The open ocean site with a water column depth of 1200 m and the back reef lagoon with a depth of 2.5 m, provided contrasting conditions to examine the environmental parameters and processes that controlled the diel cycles of DMSPCs and VOCs in tropical waters.

In the surface open ocean, vertical mixing to ca. 20 m and low nutrient concentrations (nitrate ~0.03 µM) maintained low Chla concentrations (~0.1 µg/L) and a phytoplankton assemblage dominated by Prochlorococcus, dinoflagellates and haptophytes. Despite higher DOC concentrations (~73 µM), bacterial activity was low, probably limited by nutrient scarcity and aged carbon. In these conditions, phytoplankton DMSP represented up to 3% of total particulate organic carbon and showed a marked diel variation with strongly increasing concentrations during the day, likely due to diurnal photosynthesis and photoacclimation. In such biologically unproductive waters, photochemistry ruled most of the variation of VOCs. Indeed, the concentrations of dissolved compounds known to be photochemical products, such as DMSO, COS, CS2, CH2CII, and potentially CH3I, increased with sunlight and decreased at night. The VOCs that have been more directly associated with open ocean phytoplankton, such as DMS, isoprene and bromomethanes, did not follow a clear diel pattern and occurred in concentrations at the lower end of previous observations in tropical waters. In these cases, low production rates were balanced by microbial, photochemical and atmospheric ventilation losses.

In the shallow lagoon at the back of the coral reef, the proximity of sediments, groundwater discharges, corals and abundant seaweeds resulted in higher nutrient levels (nitrate  ${\sim}0.33~\mu\text{M}),$  higher amounts of freshly produced organic matter despite lower

DOC (~69 μM), higher bacterial activity, and larger microalgal populations of weaker DMSP producers like *Synechococcus*, *Micromonas* spp., diatoms and *Cryptomonas* spp. Consequently, DMSP and DMSO concentrations were lower but those of most VOCs were higher. A combination of photobiological and photochemical processes yielded sunny-daytime increases and nighttime decreases of DMSO, DMS, DMDS, COS, isoprene, CH<sub>2</sub>CII and bromomethanes. Special mention is noted for the high concentrations of CS<sub>2</sub> (25-75 pM), probably contributed by sediments, and bromoform (290-660 pM) and dibromomethane (45-100 pM), largely contributed by seaweeds.

The interpretation of the factors governing the presence and dynamics of VOCs and DMSPCs in the two ecosystems is obviously limited by the measurements at hand. Even though we gathered a complete suite of environmental and biological variables, cause-effect links to target compound concentrations cannot be made without process studies. Having the abundances and transcripts of relevant functional genes for compound production or consumption, as well as the abundances of relevant proteins, would have been an invaluable addition to the study. Note, though, that sufficiently abundant or expressed genes have been identified for DMSPCs (Levine et al., 2012; González et al., 2019; Masdeu-Navarro et al., 2022; Tang and Liu, 2023) but not for non-DMS VOCs. For the latter, the knowledge of relevant genes and enzymes is still very poor.

Overall, in both environments, our results highlight the importance of solar radiation in DMSPC and VOC cycling through photochemical and photobiological processes. They also send a word of caution for the design of sampling strategies to study DMSPC and VOC distributions in the surface ocean and coastal ecosystems. Attention to solar time is critical to obtain measurements that are representative of the ecosystems under study over an entire diel cycle, and to allow comparison between studies.

# Data availability statement

The datasets presented in this study can be found in online repositories. The names of the repository/repositories and accession number(s) can be found below: doi: 10.5281/zenodo.10635517, https://www.ebi.ac.uk/ena, PRJEB69514, https://www.ebi.ac.uk/ena, PRJEB69515.

# **Author contributions**

RS: Conceptualization, Formal analysis, Funding acquisition, Investigation, Methodology, Resources, Supervision, Writing – original draft, Writing – review & editing. MM: Data curation, Formal analysis, Investigation, Methodology, Visualization, Writing – original draft. JM: Data curation, Investigation, Visualization, Writing – original draft, Writing – review & editing. LX: Data curation, Investigation, Writing – review & editing. MC: Data curation, Investigation, Writing – review & editing. DK: Data curation, Funding acquisition, Investigation, Writing – review & editing. PR: Data curation, Investigation, Writing – review & editing. SG: Data curation, Investigation, Writing – review & editing. SG: Data curation, Investigation, Writing – review &

editing. KB: Data curation, Investigation, Writing – review & editing. GH: Funding acquisition, Writing – review & editing. CM: Data curation, Investigation, Supervision, Writing – review & editing.

# **Funding**

The author(s) declare financial support was received for the research, authorship, and/or publication of this article. This project has received funding from the European Research Council (ERC) under the European Union's Horizon 2020 research and innovation program (grant agreement #834162, SUMMIT Advanced Grant to RS). It was also funded by the Spanish Ministry of Science and Innovation (MCIN/AEI, doi: 10.13039/501100011033) through the BIOGAPS grant (CTM2016-81008-R) to RS, the "Severo Ochoa Centre of Excellence" accreditation (CEX2019-000298-S) to the ICM, and predoctoral grants to MM-N (BES-2017-080048) and MC-B (FPU16-01925). LX and DK were supported by funding from the National Science Foundation Chemical Oceanography program (CO-1756907) to DK. SG was supported by an Australian Government Endeavour Research Fellowship. GH received funding from the Austrian Science Fund (FWF) through project ARTEMIS (P28781-B21).

# **Acknowledgments**

We thank the University of California Berkeley's Richard Gump Research station staff for kind hosting and logistical support during the field study. Thanks are also extended to Yaiza M. Castillo for flow cytometry re-analyses. Computing analyses from rDNA amplicon sequencing data were run at the Marine Bioinformatics Service of the ICM-CSIC (http://marbits.icm.csic.es).

# Conflict of interest

The authors declare that the research was conducted in the absence of any commercial or financial relationships that could be construed as a potential conflict of interest.

## Publisher's note

All claims expressed in this article are solely those of the authors and do not necessarily represent those of their affiliated organizations, or those of the publisher, the editors and the reviewers. Any product that may be evaluated in this article, or claim that may be made by its manufacturer, is not guaranteed or endorsed by the publisher.

# Supplementary material

The Supplementary Material for this article can be found online at: https://www.frontiersin.org/articles/10.3389/fmars.2024.1341619/full#supplementary-material

# References

Acuña Alvarez, L., Exton, D. A., Timmis, K. N., Suggett, D. J., and McGenity, T. J. (2009). Characterization of marine isoprene-degrading communities. *Environ. Microbiol.* 11, 3280–3291. doi: 10.1111/j.1462-2920.2009.02069.x

Amachi, S. (2008). Microbial contribution to global iodine cycling: volatilization, accumulation, reduction, oxidation and sorption of iodine. *Microbes Environ.* 23, 269–276. doi: 10.1264/isme2.ME08548

Apprill, A., Weber, L. G., and Santoro, A. E. (2016). Distinguishing between microbial habitats unravels ecological complexity in coral microbiomes. *mSystems* 1, e00143–e00116. doi: 10.1128/mSystems.00143-16

Archer, S. D., Stefels, J., Airs, R. L., Lawson, T., Smyth, T. J., Rees, A. P., et al. (2018). Limitation of dimethylsulfoniopropionate synthesis at high irradiance in natural phytoplankton communities of the Tropical Atlantic. *Limnol. Oceanogr.* 63, 227–242. doi: 10.1002/lno.10625

Balzano, S., Abs, E., and Leterme, S. (2015). Protist diversity along a salinity gradient in a coastal lagoon. *Aquat. Microb. Ecol.* 74, 263–277. doi: 10.3354/ame01740

Broadbent, A. D., and Jones, G. B. (2006). Seasonal and diurnal cycles of dimethylsulfide, dimethylsulfoniopropionate and dimethylsulfoxide at One Tree Reef lagoon. *Environ. Chem.* 3, 260–267. doi: 10.1071/EN06011

Bucciarelli, E., and Sunda, W. G. (2003). Influence of CO<sub>2</sub>, nitrate, phosphate, and silicate limitation on intracellular dimethylsulfoniopropionate in batch cultures of the coastal diatom *Thalassiosira pseudonana*. *Limnol. Oceanogr.* 48, 2256–2265. doi: 10.4319/lo.2003.48.6.2256

Burdett, H. L., Donohue, P. J. C., Hatton, A. D., Alwany, M. A., and Kamenos, N. A. (2013). Spatiotemporal variability of dimethylsulphoniopropionate on a fringing coral reef: The role of reefal carbonate chemistry and environmental variability. *PLoS One* 8, e64651. doi: 10.1371/journal.pone.0064651

Callahan, B. J., McMurdie, P. J., Rosen, M. J., Han, A. W., Johnson, A. J. A., and Holmes, S. P. (2016). DADA2: High-resolution sample inference from Illumina amplicon data. *Nat. Methods* 13, 581–583. doi: 10.1038/nmeth.3869

Carpenter, L. J., Archer, S. D., and Beale, R. (2012). Ocean-atmosphere trace gas exchange. *Chem. Soc Rev.* 41, 6473. doi: 10.1039/c2cs35121h

Carpenter, L. J., and Liss, P. S. (2000). On temperate sources of bromoform and other reactive organic bromine gases. *J. Geophys. Res.* 105, 20539–20547. doi: 10.1029/2000ID900242

Carrión, O., Li, C.-Y., Peng, M., Wang, J., Pohnert, G., Azizah, M., et al. (2023). DMSOP-cleaving enzymes are diverse and widely distributed in marine microorganisms. *Nat. Microbiol.* 8, 2326–2337. doi: 10.1038/s41564-023-01526-4

Cheng, X., Peterkin, E., and Narangajavana, K. (2007). Wastewater analysis for volatile organic sulfides using purge-and-trap with gas chromatography/mass spectrometry. *Water Environ. Res.* 79, 442–446. doi: 10.2175/106143006X111871

Coble, P. G. (1996). Characterization of marine and terrestrial DOM in seawater using excitation-emission matrix spectroscopy. *Mar. Chem.* 51, 325–346. doi: 10.1016/0304-4203(95)00062-3

Dani, K. G. S., and Loreto, F. (2017). Trade-off between dimethyl sulfide and isoprene emissions from marine phytoplankton. *Trends Plant Sci.* 22, 361–372. doi: 10.1016/j.tplants.2017.01.006

Dawson, R., Crombie, A., Pichon, P., Steinke, M., McGenity, T., and Murrell, J. (2021). The microbiology of isoprene cycling in aquatic ecosystems. *Aquat. Microb. Ecol.* 87, 79–98. doi: 10.3354/ame01972

Del Valle, D. A., Kieber, D. J., Bisgrove, J., and Kiene, R. P. (2007). Light-stimulated production of dissolved DMSO by a particle-associated process in the Ross Sea, Antarctica. *Limnol. Oceanogr.* 52, 2456–2466. doi: 10.4319/lo.2007.52.6.2456

Deschaseaux, E. S. M., Jones, G. B., Deseo, M. A., Shepherd, K. M., Kiene, R. P., Swan, H. B., et al. (2014). Effects of environmental factors on dimethylated sulfur compounds and their potential role in the antioxidant system of the coral holobiont. *Limnol. Oceanogr.* 59, 758–768. doi: 10.4319/lo.2014.59.3.0758

Deschaseaux, E., Stoltenberg, L., Hrebien, V., Koveke, E. P., Toda, K., and Eyre, B. D. (2019). Dimethylsulfide (DMS) fluxes from permeable coral reef carbonate sediments. *Mar. Chem.* 208, 1–10. doi: 10.1016/j.marchem.2018.11.008

Ekdahl, A., Pedersén, M., and Abrahamsson, K. (1998). A study of the diurnal variation of biogenic volatile halocarbons. *Mar. Chem.* 63, 1–8. doi: 10.1016/S0304-4203(98)00047-4

Exton, D. A., McGenity, T. J., Steinke, M., Smith, D. J., and Suggett, D. J. (2015). Uncovering the volatile nature of tropical coastal marine ecosystems in a changing world. *Global Change Biol.* 21, 1383–1394. doi: 10.1111/gcb.12764

Fadeev, E., Hennenfeind, J. H., Amano, C., Zhao, Z., Klun, K., Herndl, G. J., et al. (2023). Bacterial degradation of ctenophore *Mnemiopsis leidyi* organic matter. *BioRxiv*. doi: 10.1101/2023.08.14.553244

Filus, M. T., Atlas, E. L., Navarro, M. A., Meneguz, E., Thomson, D., Ashfold, M. J., et al. (2020). Transport of short-lived halocarbons to the stratosphere over the Pacific Ocean. *Atmos. Chem. Phys.* 20, 1163–1181. doi: 10.5194/acp-20-1163-2020

Fuhlbrügge, S., Quack, B., Tegtmeier, S., Atlas, E., Hepach, H., Shi, Q., et al. (2016). The contribution of oceanic halocarbons to marine and free tropospheric air over the

tropical West Pacific. Atmos. Chem. Phys. 16, 7569-7585. doi: 10.5194/acp-16-7569-2016

Galí, M., Ruiz-González, C., Lefort, T., Gasol, J. M., Cardelís, C., Romera-Castillo, C., et al. (2013a). Spectral irradiance dependence of sunlight effects on plankton dimethylsulfide production. *Limnol. Oceanogr.* 58, 489–504. doi: 10.4319/lo.2013.58.2.0489

Galí, M., and Simó, R. (2015). A meta-analysis of oceanic DMS and DMSP cycling processes: Disentangling the summer paradox. *Global Biogeochem. Cycles* 29, 496–515. doi: 10.1002/2014GB004940

Galí, M., Simó, R., Vila-Costa, M., Ruiz-González, C., Gasol, J. M., and Matrai, P. (2013b). Diel patterns of oceanic dimethylsulfide (DMS) cycling: Microbial and physical drivers. *Global Biogeochem. Cycles* 27, 620–636. doi: 10.1002/gbc.20047

Gasol, J. M., and del Giorgio, P. A. (2000). Using flow cytometry for counting natural planktonic bacteria and understanding the structure of planktonic bacterial communities. *Sci. Mar.* 64, 197–224. doi: 10.3989/scimar.2000.64n2197

Genitsaris, S., Monchy, S., Breton, E., Lecuyer, E., and Christaki, U. (2016). Small-scale variability of protistan planktonic communities relative to environmental pressures and biotic interactions at two adjacent coastal stations. *Mar. Ecol. Prog. Ser.* 548, 61–75. doi: 10.3354/meps11647

Genitsaris, S., Monchy, S., Viscogliosi, E., Sime-Ngando, T., Ferreira, S., and Christaki, U. (2015). Seasonal variations of marine protist community structure based on taxon-specific traits using the eastern English Channel as a model coastal system. FEMS Microbiol. Ecol. 91, fiv034. doi: 10.1093/femsec/fiv034

González, J. M., Hernández, L., Manzano, I., and Pedrós-Alió, C. (2019). Functional annotation of orthologs in metagenomes: a case study of genes for the transformation of oceanic dimethylsulfoniopropionate. *ISME J.* 13, 1183–1197. doi: 10.1038/s41396-019-0347-6

Grasshoff, K. (1978). Methods of seawater analysis. Proc. Anal. Div. Chem. Soc. 15, X030. doi: 10.1039/ad97815fx030

Guillou, L., Bachar, D., Audic, S., Bass, D., Berney, C., Bittner, L., et al. (2013). The Protist Ribosomal Reference database (PR2): a catalog of unicellular eukaryote small sub-unit rRNA sequences with curated taxonomy. *Nucleic Acids Res.* 41, D597–D604. doi: 10.1093/nar/gks1160

Haßler, K., Dähnke, K., Kölling, M., Sichoix, L., Nickl, A.-L., and Moosdor, N. (2019). Provenance of nutrients in submarine fresh groundwater discharge on Tahiti and Moorea, French Polynesia. *Appl. Geochem.* 100, 181–189. doi: 10.1016/j.apgeochem.2018.11.020

Happell, J. D., and Wallace, D. W. R. (1996). Methyl iodide in the Greenland/ Norwegian Seas and the tropical Atlantic Ocean: Evidence for photochemical production. *Geophys. Res. Lett.* 23, 2105–2108. doi: 10.1029/96GL01764

Hemond, E. M., and Vollmer, S. V. (2015). Diurnal and nocturnal transcriptomic variation in the Caribbean staghorn coral, *Acropora cervicornis. Mol. Ecol.* 24, 4460–4473. doi: 10.1111/mec.13320

Hench, J. L., Leichter, J. J., and Monismith, S. G. (2008). Episodic circulation and exchange in a wave-driven coral reef and lagoon system. *Limnol. Oceanogr.* 53, 2681–2694. doi: 10.4319/lo.2008.53.6.2681

Hench, J. L., and Rosman, J. H. (2013). Observations of spatial flow patterns at the coral colony scale on a shallow reef flat. *J. Geophys. Res. Oceans* 118, 1142–1156. doi: 10.1002/jgrc.20105

Hepach, H., Quack, B., Raimund, S., Fischer, T., Atlas, E. L., and Bracher, A. (2015). Halocarbon emissions and sources in the equatorial Atlantic Cold Tongue. *Biogeosci.* 12, 6369–6387. doi: 10.5194/bg-12-6369-2015

Hoadley, K. D., Hamilton, M., Poirier, C. L., Choi, C. J., Yung, C.-M., and Worden, A. Z. (2021). Selective uptake of pelagic microbial community members by Caribbean reef corals. *Appl. Environ. Microbiol.* 87, e03175–e03120. doi: 10.1128/AEM.03175-20

Hoegh-Guldberg, O., Poloczanska, E. S., Skirving, W., and Dove, S. (2017). Coral reef ecosystems under climate change and ocean acidification. *Front. Mar. Sci.* 4. doi: 10.3389/fmars.2017.00158

Hopkins, F. E., Archer, S. D., Bell, T. G., Suntharalingam, P., and Todd, J. D. (2023). The biogeochemistry of marine dimethylsulfide. *Nat. Rev. Earth Environ.* 4, 361–376. doi: 10.1038/s43017-023-00428-7

Houyun, H., Zhoy, L., Chen, J., and Taiyun, W. (2020). Extended tools for correlation analysis and visualization. Available at: https://github.com/houyunhuang/ggcor.

Howard, E. C., Henriksen, J. R., Buchan, A., Reisch, C. R., Bürgmann, H., Welsh, R., et al. (2006). Bacterial taxa that limit sulfur flux from the ocean. Science~314, 649-652. doi: 10.1126/science.1130657

Hrebien, V., Deschaseaux, E., and Eyre, B. D. (2020). Isoprene flux from permeable carbonate sediments on the Great Barrier Reef. *Mar. Chem.* 225, 103856. doi: 10.1016/j.marchem.2020.103856

Ichikawa, K., Kurihara, M., Tamegai, H., and Hashimoto, S. (2015). Decomposition of brominated organic halogens by cultures of marine proteobacteria: *Phaeobacter, Roseobacter*, and *Rhodobacter. Mar. Chem.* 176, 133–141. doi: 10.1016/j.marchem.2015.09.003

- Johnson, T. L., Palenik, B., and Brahamsha, B. (2011). Characterization of a functional vanadium-dependent bromoperoxidase in the marine cyanobacterium *Synechococcus* sp. cc93111. *J. Phycol.* 47, 792–801. doi: 10.1111/j.1529-8817.2011.01007.x
- Jones, C. E., and Carpenter, L. J. (2007). Chemical destruction of  $CH_3I$ ,  $C_2H_5I$ , 1- $C_3H_7I$ , and 2- $C_3H_7I$  in saltwater. *Geophys. Res. Lett.* 34, L13804. doi: 10.1029/2007GI 029775
- Jones, G., Curran, M., Deschaseaux, E., Omori, Y., Tanimoto, H., Swan, H., et al. (2018). The flux and emission of dimethylsulfide from the Great Barrier Reef region and potential influence on the climate of NE Australia. *J. Geophys. Res.: Atmospheres* 123, 13,835–13,856. doi: 10.1029/2018JD029210
- Jones, C. E., Hornsby, K. E., Sommariva, R., Dunk, R. M., Von Glasow, R., McFiggans, G., et al. (2010). Quantifying the contribution of marine organic gases to atmospheric iodine. *Geophys. Res. Lett.* 37, L18804. doi: 10.1029/2010GL043990
- Jones, G. B., and King, S. (2015). Dimethylsulphoniopropionate (DMSP) as an Indicator of bleaching tolerance in scleractinian corals. *J. Mar. Sci. Eng.* 3, 444–465. doi: 10.3390/jmse3020444
- Kataoka, T., Ooki, A., and Nomura, D. (2019). Production of dibromomethane and changes in the bacterial community in bromoform-enriched seawater. *Microb. Environ.* 34, 215–218. doi: 10.1264/jsme2.ME18027
- Keller, M. D., Bellows, W. K., and Guillard, R. R. L. (1989). "Dimethyl sulfide production in marine phytoplankton," in *Biogenic sulfur in the environment*. Eds. E. S. Saltzman and W. J. Cooper (American Chemical Society, Washington DC), 167–182.
- Kelly, D. P., and Smith, N. A. (1990). "Organic sulfur compounds in the environment: biogeochemistry, microbiology, and ecological aspects," in *Advances in Microbial Ecology*, vol. II. Ed. K. C. Marshall (Boston, MA: Springer), 345–385.
- Keng, F. S.-L., Phang, S.-M., Rahman, N. A., Leedham, E. C., Hughes, C., Robinson, A. D., et al. (2013). Volatile halocarbon emissions by three tropical brown seaweeds under different irradiances. *J. Appl. Phycol.* 25, 1377–1386. doi: 10.1007/s10811-013-990.x
- Keng, F. S.-L., Phang, S.-M., Rahman, Yeong, H.-Y., Malin, G., Leedham Elvidge, E., et al. (2021). Halocarbon emissions by selected tropical seaweeds exposed to different temperatures. *Phytochem.* 190, 112869. doi: 10.1016/j.phytochem.2021.112869
- Kettle, A. J. (2000). Extrapolations of the flux of dimethylsulfide, carbon monoxide, carbonyl sulfide, and carbon disulfide from the Oceans (Toronto, Ontario, Canada: Ph. D. thesis, York University).
- Kettle, A. J., Rhee, T. S., Von Hobe, M., Poulton, A., Aiken, J., and Andreae, M. O. (2001). Assessing the flux of different volatile sulfur gases from the ocean to the atmosphere. *J. Geophys. Res.* 106, 12193–12209. doi: 10.1029/2000JD900630
- Kiene, R. P. (1996). Production of methanethiol from dimethylsulfoniopropionate in marine surface waters. *Mar. Chem.* 54, 69–83. doi: 10.1016/0304-4203(96)00006-0
- Kiene, R. P., Linn, L. J., and Bruton, J. A. (2000). New and important roles for DMSP in marine microbial communities. *J. Sea Res.* 43, 209–224. doi: 10.1016/\$1385-1101(00)00023-X
- Kim, K.-H., and Andreae, M. O. (1992). Carbon disulfide in the estuarine, coastal, and oceanic environments. *Mar. Chem.* 40, 179–197. doi: 10.1016/0304-4203(92) 90022-3
- Kinsey, J. D., and Kieber, D. J. (2016). Microwave preservation method for DMSP, DMSO, and acrylate in unfiltered seawater and phytoplankton culture samples. *Limnol. Oceanogr. Methods* 14, 196–209. doi: 10.1002/lom3.10081
- Kinsey, J. D., Tyssebotn, I. M. B., and Kieber, D. J. (2023). Effect of PAR irradiance intensity on *Phaeocystis antartica* (Prymnesiophyceae) growth and DMSP, DMSO and acrylate concentrations. *J. Phycol.* 59, 963–979. doi: 10.1111/jpy.13360
- Knowlton, N., Brainard, R. E., Fisher, R., Moews, M., Plaisance, L., and Caley, M. J. (2010). "Coral reef biodiversity," in *Life in the World's Oceans*. Ed. A. D. McIntyre (Wiley- Blackwell, Oxford, UK), 65–78. doi: 10.1002/9781444325508.ch4
- Kuek, F. W. I., Motti, C. A., Zhang, J., Cooke, I. R., Todd, J. D., Miller, D. J., et al. (2022). DMSP production by coral-associated bacteria. *Front. Mar. Sci.* 9. doi: 10.3389/fmars.2022.869574
- Lawaetz, A. J., and Stedmon, C. A. (2009). Fluorescence intensity calibration using the Raman scatter peak of water. *Appl. Spectrosc.* 63, 936–940. doi: 10.1366/000370209788964548
- Lawson, C. A., Raina, J., Deschaseaux, E., Hrebien, V., Possell, M., Seymour, J. R., et al. (2021). Heat stress decreases the diversity, abundance and functional potential of coral gas emissions. *Global Change Biolol.* 27, 879–891. doi: 10.1111/gcb.15446
- Lawson, C. A., Seymour, J. R., Possell, M., Suggett, D. J., and Raina, J.-B. (2020). The volatilomes of Symbiodiniaceae-associated bacteria are influenced by chemicals derived from their algal partner. *Front. Mar. Sci.* 7. doi: 10.3389/fmars.2020.00106
- Leichter, J., Alldredge, A., Bernardi, G., Brooks, A., Carlson, C., Carpenter, R., et al. (2013). Biological and physical interactions on a tropical island Coral Reef: Transport and retention processes on Moorea, French Polynesia. *Oceanography* 26, 52–63. doi: 10.5670/oceanog.2013.45
- Lennartz, S. T., Marandino, C. A., von Hobe, M., Andreae, M. O., Aranami, K., Atlas, E., et al. (2020). Marine carbonyl sulfide (OCS) and carbon disulfide: a compilation of measurements in seawater and the marine boundary layer. *Earth Syst. Sci. Data* 12, 591–609. doi: 10.5194/essd-12-591-2020
- Lennartz, S. T., Marandino, C. A., Von Hobe, M., Cortes, P., Quack, B., Simó, R., et al. (2017). Direct oceanic emissions unlikely to account for the missing source of

atmospheric carbonyl sulfide. Atmos. Chem. Phys. 17, 385-402. doi: 10.5194/acp-17-385-2017

- Levine, N. M., Varaljay, V. A., Toole, D. A., Dacey, J. W. H., Doney, S. C., and Moran, M. A. (2012). Environmental, biochemical and genetic drivers of DMSP degradation and DMS production in the Sargasso Sea. *Environ. Microbiol.* 14, 1210–1223. doi: 10.1111/j.1462-2920.2012.02700.x
- Loreto, F., and Schnitzler, J.-P. (2010). Abiotic stresses and induced BVOCs. Trends Plant Sci. 15, 154–166. doi: 10.1016/j.tplants.2009.12.006
- Manley, S. L. (2002). Phytogenesis of halomethanes: A product of selection or a metabolic accident? *Biogeochem.* 60, 163–180. doi: 10.1023/A:1019859922489
- Manley, S. L., and Barbero, P. E. (2001). Physiological constraints on bromoform (CHBr<sub>3</sub>) production by *Ulva lactuca* (Chlorophyta). *Limnol. Oceanogr.* 46, 1392–1399. doi: 10.4319/lo.2001.46.6.1392
- Martin, M. (2011). Cutadapt removes adapter sequences from high-throughput sequencing reads.  $EMBnet\ J.\ 17,\ 10-12.\ doi:\ 10.14806/ej.17.1.200$
- Martino, M., Liss, P. S., and Plane, J. M. C. (2006). Wavelength-dependence of the photolysis of diiodomethane in seawater. *Geophys. Res. Lett.* 33, L06606. doi: 10.1029/2005GL025424
- Masdeu-Navarro, M., Mangot, J.-F., Xue, L., Cabrera-Brufau, M., Gardner, S. G., Kieber, D. J., et al. (2022). Spatial and diel patterns of volatile organic compounds, DMSP-derived compounds, and planktonic microorganisms around a tropical scleractinian coral colony. *Front. Mar. Sci.* 9. doi: 10.3389/fmars.2022.944141
- Massana, R., Murray, A. E., Preston, C. M., and DeLong, E. F. (1997). Vertical distribution and phylogenetic characterization of marine planktonic Archaea in the Santa Barbara Channel. *Appl. Environ. Microbiol.* 63, 50–56. doi: 10.1128/aem.63.1.50-56.1997
- Matsunaga, S., Mochida, M., Saito, T., and Kawamura, K. (2002). *In situ* measurement of isoprene in the marine air and surface seawater from the western North Pacific. *Atmos. Environ.* 36, 6051–6057. doi: 10.1016/S1352-2310(02)00657-X
- McGenity, T. J., Crombie, A. T., and Murrell, J. C. (2018). Microbial cycling of isoprene, the most abundantly produced biological volatile organic compound on Earth. *ISME J.* 12, 931–941. doi: 10.1038/s41396-018-0072-6
- McParland, E. L., Lee, M. D., Webb, E. A., Alexander, H., and Levine, N. M. (2021). DMSP synthesis genes distinguish two types of DMSP producer phenotypes. *Environ. Microbiol.* 23, 1656–1669. doi: 10.1111/1462-2920.15393
- Minicante, S. A., Piredda, R., Quero, G. M., Finotto, S., Bernardi Aubry, F., Bastianini, M., et al. (2019). Habitat heterogeneity and connectivity: effects on the planktonic protist community structure at two adjacent coastal sites (the lagoon and the Gulf of Venice, Northern Adriatic Sea, Italy) revealed by metabarcoding. Front. Microbiol. 10. doi: 10.3389/fmicb.2019.02736
- Modiri Gharehveran, M., and Shah, A. D. (2018). Indirect photochemical formation of carbonyl sulfide and carbon disulfide in natural waters: Role of organic sulfur precursors, water quality constituents, and temperature. *Environ. Sci. Technol.* 52, 9108–9117. doi: 10.1021/acs.est.8b01618
- Nelson, C. E., Alldredge, A. L., McCliment, E. A., Amaral-Zettler, L. A., and Carlson, C. A. (2011). Depleted dissolved organic carbon and distinct bacterial communities in the water column of a rapid-flushing coral reef ecosystem. *ISME J.* 5, 1374–1387. doi: 10.1038/ismej.2011.12
- Oksanen, J., Blanchet, F. G., Friendly, M., Kindt, R., Legendre, P., McGlinn, D., et al. (2021) vegan: Community Ecology Package. R package version 2.5-7. Available online at: https://CRANR-project.org/package=wegan
- O'Neil, J. M., and Capone, D. G. (2008). "Nitrogen cycling in coral reef environments," in *Nitrogen in the Marine Environment*. Capone, D. G., Bronk, D. A., Mulholland, M. R., and Carpenter, E. J. (Academic Press), 949–989. doi: 10.1016/B978-0-12-372522-6.00021-9
- Owens, T. G., Falkowski, P. G., and Whitledge, T. E. (1980). Diel periodicity in cellular chlorophyll content in marine diatoms. *Mar. Biol.* 59, 71–77. doi: 10.1007/BF00405456
- Parada, A. E., Needham, D. M., and Fuhrman, J. A. (2016). Every base matters: assessing small subunit rRNA primers for marine microbiomes with mock communities, time series and global field samples. *Environ. Microbiol.* 18, 1403–1414. doi: 10.1111/1462-2920.13023
- Payet, J. P., McMinds, R., Burkepile, D. E., and Vega Thurber, R. L. (2014). Unprecedented evidence for high viral abundance and lytic activity in coral reef waters of the South Pacific Ocean. *Front. Microbiol.* 5. doi: 10.3389/fmicb.2014.00493
- Pruesse, E., Quast, C., Knittel, K., Fuchs, B. M., Ludwig, W., Peplies, J., et al. (2007). SILVA: a comprehensive online resource for quality checked and aligned ribosomal RNA sequence data compatible with ARB. *Nucleic Acids Res.* 35, 7188–7196. doi: 10.1093/nar/gkm864
- Pucher, M., Wünsch, U., Weigelhofer, G., Murphy, K., Hein, T., and Graeber, D. (2019). staRdom: Versatile software for analyzing spectroscopic data of dissolved organic matter in R. *Water* 11, 2366. doi: 10.3390/w11112366
- Quack, B., and Wallace, D. W. R. (2003). Air-sea flux of bromoform: Controls, rates, and implications: air-sea flux of bromoform. *Global Biogeochem. Cycles* 17, 1023. doi: 10.1029/2002GB001890
- Raina, J.-B., Tapiolas, D. M., Lutz, A., Abrego, D., Ceh, J., Seneca, F. O., et al. (2013). DMSP biosynthesis by an animal and its role in coral thermal stress response. *Nature* 502, 677–680. doi: 10.1038/nature12677
- Ramond, P., Siano, R., and Sourisseau, M. (2018). Functional traits of marine protists. SEANOE. doi: 10.17882/51662

Ramond, P., Sourisseau, M., Simon, N., Romac, S., Schmitt, S., Rigaut-Jalabert, F., et al. (2019). Coupling between taxonomic and functional diversity in protistan coastal communities. *Environ. Microbiol.* 21, 730–749. doi: 10.1111/1462-2920.14537

R Development Core Team (2021) R: A language and environment for statistical computing. Available online at: http://www.r-project.org/.

Richter, U., and Wallace, D. W. R. (2004). Production of methyl iodide in the tropical Atlantic Ocean. *Geophys. Res. Lett.* 31, L23S03. doi: 10.1029/2004GL020779

Royer, S.-J., Galí, M., Mahajan, A. S., Ross, O. N., Pérez, G. L., Saltzman, E. S., et al. (2016). A high-resolution time-depth view of dimethylsulphide cycling in the surface sea. *Sci. Rep.* 6, 32325. doi: 10.1038/srep32325

Saint-Macary, A. D., Marriner, A., Barthelmeß, T., Deppeler, S., Safi, K., Costa Santana, R., et al. (2023). Dimethyl sulfide cycling in the sea surface microlayer in the southwestern Pacific – Part 1: Enrichment potential determined using a novel sampler. *Ocean Sci.* 19, 1–15. doi: 10.5194/os-19-1-2023

Samo, T. J., Smriga, S., Malfatti, F., Sherwood, B. P., and Azam, F. (2014). Broad distribution and high proportion of protein synthesis active marine bacteria revealed by click chemistry at the single cell level. *Front. Mar. Sci.* 1. doi: 10.3389/fmars.2014.00048

Scheffers, S. R., Nieuwland, G., Bak, R. P. M., and Van Duyl, F. C. (2004). Removal of bacteria and nutrient dynamics within the coral reef framework of Curaçao (Netherlands Antilles). *Coral Reefs* 23, 413–422. doi: 10.1007/s00338-004-0400-3

Schneider, K., Levy, O., Dubinsky, Z., and Erez, J. (2009). *In situ* diel cycles of photosynthesis and calcification in hermatypic corals. *Limnol. Oceanogr.* 54, 1995–2002. doi: 10.4319/lo.2009.54.6.1995

Simó, R., Archer, S. D., Pedrós-Alió, C., Gilpin, L., and Stelfox-Widdicombe, C. E. (2002). Coupled dynamics of dimethylsulfoniopropionate and dimethylsulfide cycling and the microbial food web in surface waters of the North Atlantic. *Limnol. Oceanogr.* 47, 53–61. doi: 10.4319/lo.2002.47.1.0053

Simó, R., Cortés-Greus, P., Rodríguez-Ros, P., and Masdeu-Navarro, M. (2022). Substantial loss of isoprene in the surface ocean due to chemical and biological consumption. *Commun. Earth Environ.* 3, 20. doi: 10.1038/s43247-022-00352-6

Simó, R., and Vila-Costa, M. (2006). Ubiquity of algal dimethylsulfoxide in the surface ocean: Geographic and temporal distribution patterns. *Mar. Chem.* 100, 136–146. doi: 10.1016/j.marchem.2005.11.006

Slezak, D., Kiene, R. P., Toole, D. A., Simó, R., and Kieber, D. J. (2007). Effects of solar radiation on the fate of dissolved DMSP and conversion to DMS in seawater. *Aquat. Sci.* 69, 377–393. doi: 10.1007/s00027-007-0896-z

Sommaruga, R., Hofer, J. S., Alonso-Sáez, L., and Gasol, J. M. (2005). Differential sunlight sensitivity of picophytoplankton from surface Mediterranean coastal waters. *Appl. Environ. Microbiol.* 71, 2154–2157. doi: 10.1128/AEM.71.4.2154-2157.2005

Stefels, J. (2000). Physiological aspects of the production and conversion of DMSP in marine algae and higher plants. J. Sea Res. 43, 183–197. doi: 10.1016/S1385-1101(00)00030-7

Stefels, J., Steinke, M., Turner, S. M., Malin, G., and Belviso, S. (2007). Environmental constraints on the production and removal of the climatically active gas dimethylsulphide (DMS) and implications for ecosystem modelling. *Biogeochemistry* 83, 245–275. doi: 10.1007/s10533-007-9091-5

Sunda, W., Kieber, D. J., Kiene, R. P., and Huntsman, S. (2002). An antioxidant function for DMSP and DMS in marine algae. *Nature* 418, 317–320. doi: 10.1038/nature00851

Swan, H. B., Crough, R. W., Vaattovaara, P., Jones, G. B., Deschaseaux, E. S. M., Eyre, B. D., et al. (2016). Dimethyl sulfide and other biogenic volatile organic compound emissions from branching coral and reef seawater: potential sources of secondary aerosol over the Great Barrier Reef. *J. Atmos. Chem.* 73, 303–328. doi: 10.1007/s10874-016-9327-7

Tang, K., and Liu, L. (2023). Bacteria are driving the ocean's organosulfur cycle. Trends Microbiol. 31, 772–775. doi: 10.1016/j.tim.2023.05.003

Thume, K., Gebser, B., Chen, L., Meyer, N., Kieber, D. J., and Pohnert, G. (2018). The metabolite dimethylsulfoxonium propionate extends the marine organosulfur cycle. *Nature* 563, 412–415. doi: 10.1038/s41586-018-0675-0

Tyssebotn, I. M. B., Kinsey, J. D., Kieber, D. J., Kiene, R. P., Rellinger, A. N., and Motard-Côté, J. (2017). Concentrations, biological uptake, and respiration of dissolved acrylate and dimethylsulfoxide in the northern Gulf of Mexico. *Limnol. Oceanogr.* 62, 1198–1218. doi: 10.1002/lno.10495

Uher, G., and Andreae, M. O. (1997). The diel cycle of carbonyl sulfide in marine surface waters: Field study results and a simple model.  $Aquat.\ Geochem.\ 2,\ 313-344.\ doi:\ 10.1007/BF00115975$ 

Wahman, D. G., Henry, A. E., Katz, L. E., and Speitel, G. E. (2006). Cometabolism of trihalomethanes by mixed culture nitrifiers. *Water Res.* 40, 3349–3358. doi: 10.1016/j.watres.2006.07.033

Wang, Q., Garrity, G. M., Tiedje, J. M., and Cole, J. R. (2007). Naïve Bayesian classifier for rapid assignment of rRNA sequences into the new bacterial taxonomy. *Appl. Environ. Microbiol.* 73, 5261–5267. doi: 10.1128/AEM.00062-07

Washburn, L., and Brooks, A. (2022). Moorea coral reef LTER, coral reef: gump station meteorological data. doi: 10.6073/PASTA/6D30349193252011BED853AE421D8B0D

Williamson, C. J., Kupc, A., Axisa, D., Bilsback, K. R., Bui, T., Campuzano-Jost, P., et al. (2019). A large source of cloud condensation nuclei from new particle formation in the tropics. *Nature* 574, 399–403. doi: 10.1038/s41586-019-1638-9

Wu, R., Vereecken, L., Tsiligiannis, E., Kang, S., Albrecht, S. R., Hantschke, L., et al. (2021). Molecular composition and volatility of multi-generation products formed from isoprene oxidation by nitrate radical. *Atmos. Chem. Phys.* 21, 10799–10824. doi: 10.5194/acp-21-10799-2021

Xie, H., Moore, R. M., and Miller, W. L. (1998). Photochemical production of carbon disulphide in seawater.  $J.\ Geophys.\ Res.\ 103, 5635–5644.\ doi: 10.1029/97JC02885$ 

Xie, H., Scarratt, M. G., and Moore, R. M. (1999). Carbon disulphide production in laboratory cultures of marine phytoplankton. *Atmos. Environ.* 33, 3445-3453. doi: 10.1016/S1352-2310(98)00430-0

Xue, L., Kieber, D. J., Masdeu-Navarro, M., Cabrera-Brufau, M., Rodríguez-Ros, P., Gardner, S. G., et al. (2022). Concentrations, sources, and biological consumption of acrylate and DMSP in the tropical Pacific and coral reef ecosystem in Mo'orea, French Polynesia. *Front. Mar. Sci.* 9. doi: 10.3389/fmars.2022.911522

Yamamuro, M., and Kayanne, H. (1995). Rapid direct determination of organic carbon and nitrogen in carbonate-bearing sediments with a Yanaco MT-5 CHN analyzer. *Limnol. Oceanogr.* 40, 1001–1005. doi: 10.4319/lo.1995.40.5.1001

Yokouchi, Y., Ooki, A., Hashimoto, S., and Itoh, N. (2014). "A study on the production and emission of marine-derived volatile halocarbons," in *Western Pacific Air-Sea Interaction Study*. Eds. M. Uematsu, Y. Yokouchi, Y. Watanabe, S. Takeda and Y. Yamanaka (Tokyo: TERRAPUB), 1–25. doi: 10.5047/w-pass.a01.001